Molecular Plant Pathology

The mitochondrial membrane protein FgLetm1 regulates mitochondrial integrity, production of endogenous reactive oxygen species and mycotoxin biosynthesis in Fusarium graminearum

Journal:	*Molecular Plant Pathology*
Manuscript ID	MPP-OA-17-227.R2
Manuscript Type:	Original Article
Date Submitted by the Author:	n/a
Complete List of Authors:	Tang, Guangfei; Institute of Biotechnology, Zhejiang University, 310058 Zhang, Chengqi; Institute of Biotechnology, Zhejiang University, 310058; College of Plant Protection, Anhui Agricultural University, 230036 Ju, Zhenzhen; Institute of Biotechnology, Zhejiang University, 310058 Zheng, Shiyu; Institute of Biotechnology, Zhejiang University, 310058 Wen, Ziyue; Institute of Biotechnology, Zhejiang University, 310058 Xu, Sunde; Institute of Biotechnology, Zhejiang University, 310058 Chen, Yun; Institute of Biotechnology, Zhejiang University, 310058 Ma, Zhonghua; Institute of Biotechnology, Zhejiang University, 310058
Keywords:	Fusarium graminearum, Endogenous reactive oxygen species, FgLetm1, Mitochondrial integrity, Mycotoxin, Virulence

The mitochondrial membrane protein FgLetm1 regulates mitochondrial integrity, production of endogenous reactive oxygen species and mycotoxin biosynthesis in *Fusarium graminearum*

Guangfei Tang[1†], Chengqi Zhang[1,2†], Zhenzhen Ju[1], Shiyu Zheng[1], Ziyue Wen[1], Sunde Xu[1], Yun Chen[1*] and Zhonghua Ma[1]

[1] Institute of Biotechnology, Zhejiang University, Hangzhou, 310058, China

[2] College of Plant Protection, Anhui Agricultural University, Hefei 230036, China

***Corresponding author:**

Yun Chen

Email: chenyun0927@zju.edu.cn;

Tel. & Fax (+86) 571 88982106.

† These authors contributed equally to this work.

RUNNING TITLE:

Function of FgLetm1 in *Fusarium graminearum*

KEYWORDS:

Fusarium graminearum; Endogenous reactive oxygen species; FgLetm1; Mitochondrial integrity; Mycotoxin; Virulence.

Word count: 6997; Figure number: 8; Table number: 3.

SUMMARY

Deoxynivalenol (DON) is a mycotoxin produced in cereal crops infected with *Fusarium graminearum*. DON poses a serious threat to human and animal health and is a critical virulence factor. Various environmental factors including reactive oxygen species (ROS) have been shown to interfere with DON biosynthesis in this pathogen. The regulatory mechanisms of how ROS trigger DON production have been extensively investigated in *F. graminearum*. However, the role of the endogenous ROS generating system in DON biosynthesis is largely unknown. In this study, we genetically analyzed the function of Leucine zipper–EF-hand–containing trans-membrane 1(LETM1) super-family proteins and evaluated the role of the mitochondria-produced ROS in DON biosynthesis. Our results show that there are two Letm1 orthologs, FgLetm1 and FgLetm2, in *F. graminearum*. FgLetm1 is localized to the mitochondria and is essential for mitochondrial integrity, whereas FgLetm2 plays a minor role in maintaining mitochondrial integrity. The ΔFgLetm1 mutant demonstrated a vegetative growth defect, abnormal conidia and increased sensitivity to various stress agents. More importantly, the ΔFgLetm1 mutant showed significantly reduced levels of endogenous ROS, decreased DON biosynthesis and attenuated virulence *in planta*. To our knowledge, this is the first report that mitochondrial integrity and endogenous ROS production by mitochondria are important for DON production and virulence in *Fusarium* species.

INTRODUCTION

Deoxynivalenol (DON) is the most prevalent and economically important mycotoxin associated with infested grains by *Fusarium* species (Desjardins, 2006). Among the *Fusarium* fungi, *Fusarium graminearum* is the main DON producer that causes a devastating disease known as Fusarium Head Blight (FHB) in cereal crops worldwide (Bennett & Klich, 2003, Desjardins, 2006, Kimura *et al.*, 2007). The biosynthetic pathway of DON has been extensively studied, and nearly all genes involved in DON biosynthesis (*TRI* genes) have been identified (Desjardins *et al.*, 1993, Kimura *et al.*, 2001, Kimura et al., 2007). Biosynthesis of secondary metabolites including mycotoxins is influenced by various environmental factors. Previous investigations on the regulation of DON biosynthesis in *F. graminearum* revealed the influence of mycotoxin production by environmental or extra-cellular factors, such as nitrogen and carbon sources (Jiao *et al.*, 2008, Miller & Greenhalgh, 1985, Oh *et al.*, 2016), pH (Merhej *et al.*, 2011), magnesium (Pinson-Gadais *et al.*, 2009), phenolic acids (Boutigny *et al.*, 2009), and amines (Gardiner *et al.*, 2009). Our recent study showed that methylation of histone H3K4 also contributed to DON production (Liu *et al.*, 2015). In addition to those factors, reactive oxygen species (ROS) have been highlighted as a stimulator interfering with DON production (Audenaert *et al.*, 2010, Ponts *et al.*, 2007, Ponts *et al.*, 2006, Montibus *et al.*, 2013, Jiang *et al.*, 2015). Supplementation with hydrogen peroxide (H_2O_2) or the fungicide prothioconazole to the liquid cultures of *F. graminearum* were able to significantly increase the concentration of intracellular ROS, which subsequently stimulated *TRI* gene expression and induced DON production (Audenaert *et al.*, 2010, Ponts *et al.*, 2007, Ponts *et*

al., 2006). Relatively higher concentrations of H_2O_2 were observed in the infection cushions, as compared to runner hyphae during the infection process of *F. graminearum* (Mentages & Bormann, 2015). However, the mechanism to generate endogenous ROS, and the role of ROS the regulation of DON biosynthesis remain relatively unknown in *F. graminearum*.

ROS are able to cause DNA damage, lipid peroxidation, and protein oxidation (Beckman & Ames, 1998). Alternatively, ROS have been suggested to be a secondary messenger that transduces signals to regulate cellular functions such as immunity, cell proliferation and ion transport in mammals and plants. In microbial eukaryotes, ROS have been shown to be involved in regulation of life-span (Osiewacz, 2002), host-pathogen interactions and other cellular functions (Missall *et al.*, 2004, Nowikovsky *et al.*, 2004). Mitochondria are the major source of endogenous ROS, and produce about 95% of the total of ROS during cellular oxidative metabolism (Liu, 1999). Meanwhile, several enzymatic and non-enzymatic systems are also involved in intracellular ROS production (Grissa *et al.*, 2010). The most important enzymatic ROS-generating system is the NADPH-dependent oxidase complex (Nox). The role of NADPH oxidases NoxA and NoxB and the regulator NoxR in ROS production have been investigated in *F. graminearum* (Wang *et al.*, 2014, Zhang *et al.*, 2016). However, the roles of mitochondria and the mitochondrial ROS-generating system in secondary metabolism and virulence of phytopathogenic fungi, including *F. graminearum,* have not been investigated.

Leucine zipper–**E**F-hand–containing **t**rans**m**embrane 1(LETM1), an inner mitochondrial membrane protein, has been identified as a protein associated with Wolf-Hirschhorn syndrome (WHS), a complex multigenic human disease

caused by the partial deletion of the distal short arm of chromosome 4 (Endele *et al.*, 1999, Zollino *et al.*, 2003). Letm1 is evolutionarily conserved from yeast to mammals. The biological functions of the Letm1 orthologs have been investigated in various organisms (Dimmer *et al.*, 2008, Hasegawa & van der Bliek, 2007, Hashimi *et al.*, 2013, McQuibban *et al.*, 2010, Nowikovsky et al., 2004, Zhang *et al.*, 2012). However, the function of the Letm1 super-family in filamentous fungi is still largely unknown. In this study, the Letm1 orthologs were selected as target proteins to investigate the biological function of ROS generated from mitochondria and mitochondrial integrity in DON biosynthesis, virulence and cell development. Our results showed that the deletion mutant ΔFgLetm1 had a vegetative growth defect and abnormal conidia. The mutant was also more sensitive to various stress agents. More importantly, ΔFgLetm1 significantly reduced the levels of cellular ROS, decreased DON biosynthesis and attenuated virulence *in planta*.

RESULTS

Identification and sequence analysis of Letm1-like proteins in *Fusarium graminearum*

A BLASTP search using *Saccharomyces cerevisiae* Letm1 family proteins, Mdm38 and Ylh47, as queries in the *F. graminearum* genome revealed only one putative Letm1 gene in this fungus, FGSG_09158 (designated as FgLetm1). The *FgLETM1* gene is predicted to encode a protein with 550 amino acids, sharing 47% and 45% sequence identity with Mdm38 and Ylh47, respectively. Meanwhile, we retrieved other genes with the LETM1 super-family domain in the *F. graminearum* genome, and found that the

FGSG_10063 locus (designated as FgLetm2) also contained a LETM1 super-family domain. However, FgLetm2 shares very low sequence identity with Mdm38 and Ylh47 (9.8% and 11.4%, respectively). Similar to *S. cerevisiae* Letm1 orthologs, FgLetm1 contains a noncanonical Letm1 protein structure with a Letm1 super-family domain, a transmembrane (TM) domain and a coiled-coil domain at the carboxyl terminus. The FgLetm2 protein harbors a truncated Letm1 super-family domain after the TM domain at the carboxyl terminus (Fig. 1a). Both FgLetm1 and FgLetm2 lack the EF-hand domain present in human Letm1 (NP_036450). This was consistent with a previous study, in which it was demonstrated that the EF-hand domain was absent in lower eukaryotes, fungi and plasmodium (Nowikovsky et al., 2004).

To gain more insight into the Letm1 evolution in fungi, we retrieved all genes that encode proteins containing the Letm1 super-family domain from 32 fungal genomes available in the NCBI Bioprojects and Broad Institute database. The results indicated that genes for the Letm1-like proteins are highly conserved in fungi, while the number of orthologs varies in different fungal species. Most fungal species (25 out 32) harbored two orthologs, albeit the representative fungi from *Taphrinomycotina*, *Pucciniomycotina* and *Chytridiomycota* contained only one Letm1-like protein. Moreover, three different genes encoding the Letm1-like proteins were retrieved from *Zygomycota* fungi *Rhizopus oryzae* and *Mucor circinelloides* (Fig. S1). A phylogenetic analysis of the putative Letm1-like proteins, which include *F. graminearum* and six filamentous phytopathogenic fungi, showed that the Letm1-like proteins are significantly divided into two groups (Fig. 1b). Proteins in group II had a truncated Letm1 super-family domain with a length of 58-75

amino acids (Table S1). The domain characteristic and the phylogenetic tree indicated that FgLetm1 might have similar biological functions to the Letm1 proteins Mdm38 and Yln47 in *S. cerevisiae*.

In addition, our in-house RNA-seq data indicated that the transcriptional level of *FgLETM1* was higher than that of *FgLETM2*, by a range of 5- to 20-fold higher, in all four tested conditions including in the conidiation medium (CMC), hyphae grown in PDA, plant infection and deoxynivalenol (DON) biosynthesis induction medium (TBI) (Fig. 1c).

Disruption of FgLetm1 and FgLetm2

To characterize the function of FgLetm1 and FgLetm2, we generated single and double deletion mutants, ΔFgLetm1, ΔFgLetm2 and ΔΔFgLetm1/2, using the homologous recombination strategy. The single or double deletion mutants were confirmed by Southern hybridization assays (Fig. S2). To confirm that the phenotypic abnormalities of the mutants were directly related to the deletion, we complemented the deletion mutants with the gene fused with *gfp* for the green florescent protein (GFP) at the carboxyl terminus under their native promoters, respectively, and generated the complemented strain ΔFgLetm1-C (ΔFgLetm1+P_{LETM1} FgLetm1-GFP) and ΔFgLetm2-C (ΔFgLetm2+P_{LETM2} FgLetm2-GFP) . The complemented strains were also confirmed by Southern blot assays and PCR amplification (Fig. S2).

FgLetm1 regulates hyphal growth, conidiation and conidial germination

The ΔFgLetm1 mutant demonstrated radial and hyphal growth defects. The rate of radial growth of ΔFgLetm1 was reduced on both PDA (potato dextrose agar) and MM (minimal medium), in comparison with that of wild type PH-1, respectively. Moreover, the deletion mutant of ΔFgLetm1 exhibited a reduction

in aerial hyphae formation on solid agar plates (Fig. 2 a).

ΔFgLetm1 produced less conidia than that of the wild type PH-1 after 4 days of incubation in CMC (Table 1). To further examine conidial morphology, calcofluor white staining assays were performed for individual mutants. The results were observed under the fluorescent microscope. As shown in Fig. S3 and Table 1, the size of conidia produced by ΔFgLetm1 was shorter, in comparison with that of the wild type. Moreover, the conidia of ΔFgLetm1 harbored fewer septa. Most of the conidia (65%) had only 3 septa in the ΔFgLetm1, while the majority of conidia produced by wild type had 5 septa (Fig. 2b). Meanwhile, the abnormal conidia of ΔFgLetm1 showed slower germination than that of the wild type in the present of 2% sucrose (Fig. 2c).

In contrast, the deletion mutant of ΔFgLetm2 did not show visible phenotypic differences in vegetative growth, conidia formation and germination, in comparison with that of the wild type. The ΔΔFgLetm1/2 double mutant demonstrated similar phenotypes as those in the ΔFgLetm1 single mutant. Phenotypic defects of ΔFgLetm1 were restored by the complementation in the complemented strain ΔFgLetm1-C (Fig. 2). Thus, our evidences confirmed that the defects in the mutants were linked to the loss of the *FgLETM1* gene. Taken together, the data presented here suggested that FgLetm1 is involved in the hyphal growth, conidiation and conidial germination, and that FgLetm2 playes a dispensable role in these biological processes under the tested conditions.

Deletion mutant of ΔFgLetm1 showed increased sensitivity towards osmotic stress, heat shock and fungicides

It has been reported that Mdm38 is involved in resistance to several biotic stresses in yeast (Frazier *et al.*, 2006, Sinha *et al.*, 2008, Dimmer *et al.*, 2002a).

Therefore, we were interested in determining the susceptibility of the mutants in *F. graminearum* to various stresses, including osmotic stress, heat shock, and fungicide treatment. The susceptibility assays showed that the ΔFgLetm1 mutant had a significantly increased sensitivity to osmotic stresses generated by NaCl or KCl, whereas the ΔFgLetm2 mutant displayed the same susceptibility to that of the wild type towards osmotic stresses (Figs. 3a, b). The heat tolerance of the mutants was examined at 15 °C, 25 °C and 32 °C. As shown in Fig. 3c, all strains displayed similar growth rate as that of the wild type at 15 °C. For growth at 32 °C, noticeably, the ΔFgLetm1 mutant could not grow at 32 °C. The complemented strains had similar growth rate and colony morphology with the wild type PH-1. Therefore, our results indicated that ΔFgLetm1 increased sensitivity to heat shock stress. To further confirm the increase of sensitivity to high temperatures in ΔFgLetm1, we assayed the transcriptional levels of the *FgHSP30* (Fg01158), *FgHSP70* (Fg00838), and *FgGSY2*(Fg06822) genes, whose products are involved in the heat shock tolerance in *F. graminearum* (Hu et al., 2014). When cultures were shifted from 25°C to 32°C for 1 h, the relative expression levels of *FgHSP70* and *FgHSP30* were 2.5- and 2-fold higher, respectively, in PH-1 compared to that of ΔFgLetm1 (Fig. 3d). Therefore, the deletion mutant of ΔFgLetm1 decreased the expression of the selected heat stress response genes in *F. graminearum*.

The susceptibility of the mutants towards ions and fungicides were also examined. ΔFgLetm1 displayed more sensitivity to iprodione, phenamacril, $FeSO_4$ and $CaCl_2$ than that of the wild type and complemented strains (Fig. 3e, f). In particular, the ΔFgLetm1 mutant was hyper-sensitive to Fe^{2+} and could not grow on the MM amended with 10 mM Fe^{2+}. It implied that FgLetm1 might

regulate the ferrum homeostasis in this fungus. The double mutant ΔΔFgLetm1/2 showed similar phenotypes with that of ΔFgLetm1 in all tested conditions.

FgLetm1 is localized to the mitochondria and is critical for mitochondrial integrity

The complemented strains ΔFgLetm1-C and ΔFgLetm2-C with GFP-fusion proteins were rescued for the phenotypice defects seen in the mutants (Figs. 2-3), indicating that the fusion proteins were functional. These strains were further used for observing the subcellular localization of FgLetm1 and FgLetm2. A filamentous network pattern of GFP signals was present in the vegetative mycelia of the ΔFgLetm1-C strain (Fig. 4a). Co-localization experiments were performed using dual-labeling with FgLetm1-GFP and mitochondrial indicator Mito-HcRed staining. As shown in Fig. 4a, the GFP and Mito-HcRed signals clearly overlapped, suggesting that FgLetm1 was localized to the mitochondria. Using the same assay, we observated that FgLetm2-GFP was also co-localized with Mito-HcRed (Fig. 4a). Therefore, both FgLetm1 and FgLetm2 were localized to the mitochondria.

Since both FgLetm1 and FgLemt2 were shown to be mitochondria localized proteins, we were interested in testing whether the deletion mutants would show altered mitochondrial structures. First, the mitochondrial patterns were observed by Mito-HcRed staining. Mito-HcRed signal in the mycelia of PH-1 and the complemented strains dominantly showed the filamentous network shapes (Fig. 4b, video S1), while it displayed punctate patterns in the mycelia of the ΔFgLetm1 single and the double mutant (Fig. 4b, video S2). Interestingly, mitochodrial mobility was relatively slower in the ΔFgLetm1

mutant than in the wild type (videos S1, S2). This implied that the mitochondrial morphology and function might be different in PH-1 and ΔFgLetm1. Next, transmission electron microscope (TEM) experiment was applied to visualize the details of the mitochondrial structures. The TEM micrographs revealed that the deletion of the *FgLETM1* gene caused mitochondrial swelling, an increase in mitochondrial volume and a lack of tubular shaped cristae structures (Fig. 4c). The mitochondrial morphologies in the ΔFgLetm2 cells showed similar shape and cristae structures in comparison with that in PH-1, while the volume was slightly increased. The abnormal mitochondrial morphologies of the double mutant were consistent with those of the ΔFgLetm1 mutant (Figs. 4b, c).In yeast, Mdm38 is essential for the biosynthesis of the respiratory chain components (Frazier et al., 2006). To test whether FgLetm1 has a similar function in *F. graminearum*, we selected cytochrome *b* (Cyt *b*) as the indicator protein of respiratory chain components, and detected the protein level of Cytb by western blotting. As shown in Fig. 4d, the abundance of the Cyt *b* protein was clearly decreased in ΔFgLetm1 and the double mutant. Our findings thus strongly suggested that FgLetm1 is a structural protein, which helps to maintain the mitochondrial structure and is essential for the biosynthesis or the stability of the components in the respiratory chain, whereas FgLetm2 might play a minor role in these processes.

The deletion mutant of ΔFgLetm1 decreased the production of endogenous ROS and reduced ATP biosynthesis

Mitochondria are an important source of ATP synthesis and ROS production in eukaryotic cells. Given that the deletion mutant of ΔFgLetm1 resulted in

mitochondrial dysfunction, we next compared the concentration of intracellular ROS and ATP biosynthesis in all above strains. The ROS content was qualitatively analyzed with H2DCFDA (2', 7'-dichlorodihydrofluorescein diacetate) staining in MM and TBI. As indicated in Fig. 5a, the mycelia of the wild type, ΔFgLetm2 and complemented strains were all stained by the dye and cells showed green signals under fluorescent microscope. Interestingly, mycelia of the wild type, ΔFgLetm2 and complemented strains were swelled and formed ovoid toxigenic cells, and displayed noticeably stronger green signals in TBI (Fig. 5a, bottom panel) than in MM (Fig. 5a, upper panel). These results suggested that ROS production were highly induced and ROS was accumulated in cells during DON biosynthesis. However, limited fluorescent signals were detected in ΔFgLetm1 and the double mutant in both media (Fig. 5a). Quantification data also confirmed that endogenous ROS was significantly reduced in ΔFgLetm1 and ΔΔFgLetm1/2 (Table 2). Intracellular ROS levels are usually balanced by the activities of catalases and superoxide dismutases. Therefore, we performed qRT-PCR to measure the transcripts of seven putative catalase and superoxide dismutase genes in the mycelia of the wild type and the ΔFgLetm1 mutant after 3 days of incubation in TBI. As expected, the qRT-PCR results indicated that all selected genes, except for *FgZnSOD2*, showed very low transcriptional levels in ΔFgLetm1 in response to limited intracellular ROS-mediated oxidative stress, in comparison with their expression levels in the wild type (Fig. 5b). To determine whether the reduction of intercellular ROS in ΔFgLetm1 and the double mutant would lead to their higher tolerance towards extracellular ROS stress, we measured the sensitivity of all strains to oxidative stress on the MM supplemented with 10 mM H_2O_2.

Deletion mutant of ΔFgLetm1 and the double mutant exhibited significantly increased tolerance to oxidative stress mediated by H_2O_2 compared to that of the wild type, ΔFgLetm2 and complemented strains (Fig. 5c, d).

We next measured ATP production in the deletion mutants. The quantification data indicated that the production of ATP in the ΔFgLetm1 and the double mutant was decreased about 30%, compared with that of the wild type. The ΔFgLetm2 mutant and the complemented strains produced ATP at a level similar to that of the wild type strain (Table 2). In mammals, LETM1 knock-down led to mitochondrial malfunction and an induction of glycolysis in the cytoplasm to maintain their ATP supply in these cells (Dimmer et al., 2008, Hwang *et al.*, 2010). To investigate whether the dysfunctional mitochondria in ΔFgLetm1 also increases glycolysis, we measured the concentration of ethanol, the byproduct of anaerobic respiration in fungi, in MM after 16 h of incubation. As expected, the ethanol concentration of the cell-free supernatant from the ΔFgLetm1 mutant was significantly elevated compared to the wild type (Table 2), indicating that the *FgLETM1* deletion disrupted the respiration chain and up-regulated the glycolytic pathway in *F. graminearum*. Collectively, our data suggested that FgLetm1 is critical for normal mitochondrial function in ATP generation and ROS production.

The ΔFgLetm1 mutant is significantly attenuated in virulence

On wheat heads inoculated with PH-1, or ΔFgLetm2, or the complemented strains, scab symptoms were first developed on the inoculated spikelets and rapidly spread to the whole wheat head after 15 days of inoculation. In contrast, the hyphal growth of ΔFgLetm1 or the ΔΔFgLetm1/2 double mutant failed to spread from the inoculated floret to the rachis, and subsequently caused scab

symptoms only in the inoculated spikelet (Fig. 6a, upper panel). Moreover, almost all grains in infected wheat ears by wild-type PH-1, ΔFgLetm2 and complemented strains were shriveled and bleached, while only the grain at the inoculated site was shrunken in the treatment of ΔFgLetm1 and ΔΔFgLetm1/2 (Fig. 6a, bottom panel). Since that ΔFgLetm1 and ΔΔFgLetm1/2 mutants grew well on the wheat head tissue medium (WA) (Fig. S4), the attenuated virulence of ΔFgLetm1 and ΔΔFgLetm1/2 was not likely due to the growth defect. Next, we investigated whether the deletion mutations affected the penetration process. We examined the infection structures of strains during the infection using scan electron microscope (SEM). Ultrastructural examination showed that the hyphae of the wild type formed typical infection cushions on the glumes at 48 h post-inoculation with conidia, but such penetration structures were not observed on the glumes inoculated with conidia of either ΔFgLetm1 or ΔΔFgLetm1/2 under the same conditions. Both ΔFgLetm2 and the two complemented strains showed similar infection structures on plant tissues to those of the wild type (Fig. 6b). Noticeably, the ΔFgLetm1 mutant was capable of penetrating the spikelet and resulted in the scab symptom after 2 weeks at the inoculated sites (Figs. 6a, S5). These results suggested that the ΔFgLetm1 mutant delayed the penetration structure formation and was defective in spreading from the inoculation site to nearby spikelets *via* the rachis. We conclude that FgLetm1 is important in virulence in *F. graminearum*.

FgLetm1 plays a critical role in DON biosynthesis

DON biosynthesis in the mutants was evaluated both *in vitro* and *in planta*. First, the transcriptional levels of *TRI* genes in the mutants were assayed by qRT-PCR in TBI. All selected *TRI* genes were strongly down-regulated in the

ΔFgLetm1mutant, but the expression was not affected in ΔFgLetm2, compared to those in the wild type (Fig. 7a). Next, the toxisome formation (Boenisch *et al.*, 2017) for DON biosynthesis in the wild type and the mutants was observed using the Tri1-GFP as an indicator in TBI cultures. As shown in Fig. 7b, the Tri1-GFP was highly induced and formed spherical and crescent toxisomes in the mycelia of the wild type and the ΔFgLetm2 mutant after 3 days of incubation in TBI. However, no visible green fluorescent signals were observed in the mycelia of ΔFgLetm1 under the same condition. Consistent with the expression of *TRI* genes and toxisomes formation, the amount of the final product of DON biosynthesis in ΔFgLetm1 was strongly reduced by 18-fold when compared tp that in in the wild type in the TBI liquid medium (Table 3). DON production was also significantly reduced in the ΔFgLetm1 deletion mutant in wheat grain cultures and the infested wheat kernels *in planta*. The complemented strain ΔFgLetm1-C was completely restored in DON production (Table 3). Collectively, our results suggest that FgLetm1 is important in *TRI* gene expression and DON production in *F. graminearum*.

To determine whether the DON reduction is caused by decreased ATP and ROS production in ΔFgLetm1, we conducted DON rescue assays by supplying exogenous ATP or H_2O_2 in the liquid cultures induced by ammonium as described previously (Gardiner et al., 2009). Treatment with H_2O_2 clearly increased DON biosynthesis in PH-1, and partially recovered DON biosynthesis in ΔFgLetm1(Fig. 7c). However, the final production of DON after induction by H_2O_2 was still less than in the wild type (Fig. 7c). We next assayed the expression of *TRI5*, *TRI6* and *TRI10* with RNA samples isolated from hyphae of the wild-type and ΔFgLetm1 mutant with or without treatment of 0.5

mM H_2O_2 in LTB at day 3. In the wild type strain, the expression levels of *TRI5, TRI6* and *TRI10* were 4.0-, 10.4- and 5.2-fold higher in H_2O_2-treated samples than in untreated samples (Fig. 7d). Treatment with H_2O_2 also induced the expression of these *TRI* genes in the ΔFgLetm1 mutant (Fig. 7d). However, addition of exogenous ATP in TBI was unable to rescue the decreased of DON biosynthesis in the ΔFgLetm1 mutant (Fig. S6). Therefore, our evidence implied that the diminished endogenous ROS might be partly responsible for the reduction of DON biosynthesis in ΔFgLetm1.

Wild type *F. graminearum* produced less DON and was strongly attenuated in virulence under the hypoxic condition.

Given that dysfunctional mitochondria in the ΔFgLetm1 mutant increased the activity of glycolysis, but decreased the DON biosynthesis and virulence, we speculated that DON biosynthesis might be suppressed under hypoxic condition. Therefore, we investigated DON biosynthesis and virulence of *F. graminearum* under the limited O_2 condition (1%). Surprisingly, the radial growth rate of the wild type PH-1 under hypoxic condition was similar to that under the open air condition (Fig. 8a). Compared with the expression of *TRI5*, *TRI6* and *TRI10* in TBI under the open air condition, the expression of these genes in the wild type was strongly reduced under the hypoxic condition (Fig. 8b), which was similar levels to these in ΔFgLetm1 mutant (Fig. 7a). However, the transcriptional level of the control gene *AURJ* for pigment formation was increased under the hypoxic condition, indicating that the reduction of the *TRI* gene expression was somehow specific under the hypoxic condition. Meanwhile, the Tri1-GFP labeled toxisome formation was also completely abolished under the hypoxic condition (Fig. 8c). Finally, the DON production

under hypoxic condition decreased by 40-fold than that in the open air (Fig. 8d). The pathogenicity assay was also conducted under both conditions. After 7 days post-inoculation, the mycelia were able to infect the inoculated site, caused the necrotic symptom, and spread to nearby spikelets under the open air condition (Fig. 8e, left-hand panel). Remarkably, wild type PH-1 failed to infect the inoculate spikelet under the hypoxia condition (Fig. 8e, right-hand panel). Taken together, DON biosynthesis and virulence were suppressed in *F. graminearum* under the low oxygen conditions, similar to the effect of dysfunctional mitochondria caused by deletion of the *FgLETM1* gene.

DISCUSSION

Mdm38 in yeast is critical for the maintenance of mitochondrial morphology. The lack or RNAi silencing of Letm1 orthologs led to the disruption of the mitochondrial network and apparent swelling of the mitochondria in various organisms (Dimmer *et al.*, 2002b, Nowikovsky et al., 2004, Schlickum *et al.*, 2004, Sickmann *et al.*, 2003, Hasegawa & van der Bliek, 2007, McQuibban et al., 2010, Hashimi et al., 2013). To date, no study has been conducted to investigate the biological roles of the Letm1 orthologs in filamentous fungi. In this study, we showed that the ΔFgLetm1 mutant of the filamentous fungus *F. graminearum* lacked tubular-shaped cristae structures and had increased mitochondrial volumes (Fig. 4b-c). Interestingly, for the first time, we also showed that FgLetm1 plays an important role in mitochondrial mobility, since the ΔFgLetm1 mutation slows down the dynamic change of mitochondria (Videos S1-2). Mdm38 in *S. cerevisiae* also plays a critical role in the biogenesis of the respiratory chain by coupling ribosome function to protein transport across the inner membrane (Frazier et al., 2006, Tamai *et al.*, 2008).

Here, we found that the protein synthesis of cytochrome *b* decreased in the ΔFgLetm1 mutant (Fig. 4d). To support this idea, we conducted an affinity capture assay with the FgLetm1-GFP fusion protein as a bait. Protein mass spectrometry data showed that 18 proteins of the mitochondrial ribosome were associated with FgLetm1 (Table S2). Among them, 12 homologous proteins were also found in complex with Mdm38 and Ylh47 by affinity purification in yeast (Frazier et al., 2006). Taken together, the roles of the Letm1 super-family proteins in mitochondrial integrity and the biogenesis of the respiratory chain seem to be highly conserved from yeast to mammals, although their amino acid sequence and motif features differ among each other.

In addition, we also found that FgLetm1 *in F. graminearum* had some distinct features from their orthologs in other organisms. For instance, Mdm38 is required for efficient growth on non-fermentable carbon sources, such as glycerol, in yeast (Frazier et al., 2006). In contrast, the ΔFgLetm1 mutant of *F. graminearum* showed a comparable growth phenotype on agar media supplemented with either glucose or glycerol as the sole carbon source (Fig. S7). Deletion of ΔFgLetm1 was strongly decreased the conidiation and septum of conidia, and reduced stress response towards fungicides, ions and oxidative stress. These results implied that FgLetm1 is critical for fitness in certain environmental niches. Therefore, FgLetm1 may have species-specific activities, in addition to the conserved function of Letm1 orthologs in maintaining the integrity of mitochondria.

Reactive oxygen species (ROS) play a major role in pathogen-plant interactions, during which the host plant rapidly triggers an oxidative burst to suppress a pathogen infection. Pathogens have to cope with plant-released

ROS during a successful infection (Apel & Hirt, 2004, Heller & Tudzynski, 2011). Most likely, all organisms have evolved oxidative stress response (OSR) mechanisms to scavenge elevated intracellular ROS levels. The ROS scavenging system is important for the detoxification of ROS in the cells, and the OSR has to be tightly regulated. In budding yeast, several signal components are involved in the regulation of the OSR at the transcriptional level, including the Hog1 cascade and the transcription factors Yap1, Atf1 and Skn7 (He & Fassler, 2005, Kim & Hahn, 2013, Raitt *et al.*, 2000). In *F. graminearum*, all three stress-related transcription factor genes, *FgAP1*, *FgATF1* and *FgSKN7*, play a role in the tolerance of oxidative stress. Moreover, *F. graminearum* has evolved its OSR system to transduce oxidative stress as a signal for the induction of DON biosynthesis, which is a critical virulence factor during the infection process (Jiang *et al.*, 2015, Montibus *et al.*, 2013, Van Nguyen *et al.*, 2013). A supplement of H_2O_2 in the cell culture of *F. graminearum* stimulated *TRI* gene expression and increased DON accumulation, in a manner largely dependent on the OSR transcription factor FgSKN7 (Jiang et al., 2015). In addition to treatment of exogenous ROS, endogenous ROS also modulates DON production. H_2O_2 was shown to constitutively accumulate in the DON induction medium in the culture of *F. graminearum.* Moreover, the time course curve of H_2O_2 accumulation followed the pattern of DON production (Ponts et al., 2006, Ponts et al., 2007). Consistence with above findings, we found that ROS was highly accumulated in the mycotoxin induction medium (TBI), and exogenous H_2O_2 was stimulated the DON production (Figs. 5, 7). We also found that deletion of *FgLETM1* almost completely abolished ROS production in mitochondria in MM and TBI

media (Fig. 5a, Table 2), and caused the reduction of DON biosynthesis both *in vitro* and *in planta* (Table 3). The expression of *TRI* genes and DON production in ΔFgLetm1 were partially rescued in the LTB medium supplemented with H_2O_2 (Figs. 7c-d). Therefore, the mitochondria-derived ROS was important for the DON biosynthesis in *F. graminearum*, although other factors related to mitochondrial dysfunction might also be involved in this process (Bonnighausen *et al.*, 2015).

The concentration of oxygen in the atmosphere is important for the biosynthesis of mycotoxins. *Penicillium griseofulvum* produced less of the patulin toxin in 1% or 5% O_2 environment than in open air (20% O_2) (Paster & Lisker, 1985). Ans another example, only trace amounts of T-2 toxin was detected in *Fusarium sporotrichioides* under 40% CO_2/5% O_2, in comparison with a much greater amount of T-2 toxin under 40% CO_2/20% O_2 (Paster *et al.*, 1986). Fungal growth in these gaseous environments was identical to that under the open air condition, even in O2 concentrations of <1% (Hocking, 1989).. Here we found that *F. graminearum* showed normal growth patterns in the 1% O_2 condition as in the open air condition (Fig. 8a), but low levels of oxygen strongly reduced DON production and virulence (Fig. 8b-e), similar to the phenotypes seen in the ΔFgLetm1 mutant (Figs. 6, 7). On the other hand, disruption of the mitochondrial integrity in ΔFgLetm1 significantly reduced the DON production (Fig. 7, table 3). We infer that fungicides targeting the mitochondria might possess a potential role in controlling the DON biosynthesis and FHB. We thus evaluated the effect of three mitochondrial targeting fungicides including boscalid, pyraclostrobin and py-diflumetofen on the DON production. As expected, all three tested fungicides strongly reduced

the DON production (Fig. S8). Taken together, our results suggested that storage of grain under hypoxia and fungicides targeting mitochondria might provide potential approaches for DON management.

EXPERIMENTAL PROCEDURES

Fungal strains and culture conditions

Fusarium graminearum strain PH-1 (NRRL 31084) was used as the progenitor for constructing gene deletion mutants. The wild type and transformants generated in this study were grown at 25 °C on potato dextrose agar, minimal medium, and wheat-head medium for mycelial growth tests (Liu et al., 2015). CMC media was used for sporulation assays (Cappelli.Ra & Peterson, 1965). For quantifying the DON production, strains were grown in liquid TBI medium (Menke *et al.*, 2012). To evaluate the effect of H_2O_2 on the induction of DON biosynthesis, wild type or mutants were cultured in the LTB as described (Jiang *et al.*, 2016), and H_2O_2 was supplemented at a final concentration of 0.5 mM. For hypoxia condition, the inoculated TBI or wheat heads were statically incubated in a modular incubator chamber (billups-rothenberg, Inc) filled with mixture gases (1% O_2, 99% N_2).

The sensitivity of strains towards stress agents was determined as described previously (Liu et al., 2015). The final concentration of NaCl, KCl, and fungicides, Fe^{2+}, $CaCl_2$ and H_2O_2 in MM were indicated in the figure. For testing the temperature sensitivity of the mutants, cells were grown at 15 °C, 25 °C and 32 °C. The mycelial growth inhibition rate (MGIR) was calculated using the formula MGIR% = [(N-C)/C]*100, where, C is colony diameter of the control without treatment, and N is that with treatment. Each experiment was

repeated three times independently.

Construction of gene deletion mutants and complemented strains

Construction of gene deletion and complementation vectors and subsequent transformation of *F. graminearum* were carried out using the protocols described previously (Jiang *et al.*, 2011). In order to generate double mutant of *FgLETM1* and *FgLETM2*, *FgLETM1* was knocked out in the *FgLETM2* deletion mutant (ΔFgLETM2). The primers used to amplify the flanking sequences of each gene are listed in Table S3. Deletion candidates were identified by PCR with designated primers (Table S3), and were further analyzed by Southern blotting. Three independent transformants for each mutant were used in all experiments. FgLetm1-GFP, FgLetm2-GFP, Tri1-GFP and FgAtg8-RFP fusion constructs were generated as described previously (Gu *et al.*, 2015a).

Plant infection and DON production assays

A 10-μl aliquot of conidial suspension (1×10^5 conidia/ml) was injected into a floret in the central section spikelet of single flowering wheat head of susceptible cultivar grown in the field. There were ten replicates for each strain. Fifteen days after inoculation, the infected spikelets in each inoculated wheat head were recorded. The experiment was repeated four times, and typical symptom was shown. Infectious hyphae developed in wheat tissue cells were examined at 48 h post-inoculation by SEM.

The strain expressing the Tri1-GFP was used as the fluorescent reporter strain for toxisome formation, and toxisome formation was observed after 3 days of incubation in TBI. The DON production in the wild type, the mutants and complemented strains were quantified under several conditions, including the TBI, LTB, wheat kernel medium and inoculated spikelets. The supernatant

of TBI after 7-day incubation was collected for quantification of DON. DON production in wheat kernel medium was conducted as described previously (Liu et al., 2015, Ji *et al.*, 2014). The inoculated spikelets were harvested after fifteen days, and DON was extracted as described (Jiang et al., 2015). Total amount of egrosterol was extracted from infected spikelets as described (Liu et al., 2013). For ROS induction assay, LTB was used for replacement of TBI, since the DON biosynthesis was already extremely induced. Recipe of LTB medium was modified from TBI, only replacing the putrescine to ammonium nitrate at the final concentration of 5 mM. H_2O_2 was daily added into the LTB to the final concentration of 0.5 mM. After 7 days of incubation, the supernatant was collected for DON quantification. DON samples were quantified by LC-MS/MS as described previously (Dong *et al.*, 2016). The experiment was repeated three times.

qRT-PCR assays

RNA samples of the wild type, mutants and complemented strains were isolated as described (Liu et al., 2015). For the induction of *TRI* genes by H_2O_2, the hyphae of wild type or mutant were harvested for RNA extraction after 48 h of treatment. TAKARA SYBR Premix Ex Taq was used for qRT-PCR assays with the CFX96 Real-Time System as described (Bio-RAD, USA). The actin gene of *F. graminearum* was used as the internal control. Relative expression levels of each gene were calculated with the $2^{-\Delta\Delta Ct}$ method (Livak & Schmittgen, 2001).

Western blotting hybridization

The protein extraction and Western blot analysis were performed as described previously (Yun *et al.*, 2015). Anti-MT-CYB antibody (Abcam, ab103405) was

used to detect the cytochrome b for analyzing the biosynthesis of the respiratory chain. The samples were also detected with monoclonal anti-H3 antibody (Abcam, ab1791) as a reference. The mCherry-FgAtg8 proteolysis was quantified by western blots with anti-mCherry antibody (Abcam, ab167453). The samples were also detected with monoclonal anti-GAPDH antibody EM1101 (Hangzhou HuaAn Biotechnology co., Ltd.) as a reference. All experiments were conducted three times.

Microscopy imaging

Localization of green fluorescent labeled proteins and Mito-HcRed (Thermo Fisher, M7512) staining signals were visualized by the Zeiss LSM780 confocal microscope (Carl Zeiss AG, Germany). The microstructure of mitochondria in wild type or mutants was treated as described (Yun et al., 2015) and observed by the transmission electron microscope (TEM) JEOL JEM-1230. For observation of infection structures on wheat glumes, the glumes were treated as previous described (Gu *et al.*, 2015b), and observed in Hitachi Model TM-1000 scan electron microscope (SEM) (Hitachi, Tokyo, Japan).

Quantification of ATP and H_2O_2 production

The mycelia grown in MM for 24 h and in TBI for 3 days were used for quantification of H_2O_2 and ATP. H_2O_2 and ATP production were assayed using the Hydrogen Peroxide Assay Kit (Beyotime Institute of Biotechnology, China, S0038) and ATP Assay Kit (Beyotime, S0026), respectively. Briefly, mycelia (0.05 g) were added to 200 μl of the lysis buffer in the H_2O_2 detection kit or 500 μl of the lysis buffer in the ATP detection kit. After lysis of mycelia, quantification of H_2O_2 or ATP production was conducted following the

instructions provided by the manufacturer. Experiments were repeated three times.

ACKNOWLEDGEMENTS

We thank Dr. Jiang Cong and Dr. Huiquan Liu (Northwest A&F University) for DON quantification and bioinformatics analyses, Prof. Yunrong Chai (Northeastern University, Boston) and Kevin Gozzi (Massachusetts Institute of Technology) for manuscript editing. The research was supported by the Natural Science Foundation of Zhejiang Province (LR17C140001), National Natural Science Foundation of China (31672064), International Science & Technology Cooperation Program of China (2016YFE0112900) and China Agriculture Research System (CARS-3-1-15). The authors declare no conflict of interest.

REFERENCES

Apel, K. and Hirt, H. (2004) Reactive oxygen species: Metabolism, oxidative stress, and signal transduction. *Annu Rev Plant Biol,* **55,** 373-399.

Audenaert, K., Callewaert, E., Hofte, M., De Saeger, S. and Haesaert, G. (2010) Hydrogen peroxide induced by the fungicide prothioconazole triggers deoxynivalenol (DON) production by *Fusarium graminearum*. *BMC Microbiol,* **10**.

Beckman, K. B. and Ames, B. N. (1998) The free radical theory of aging matures. *Physiol Rev,* **78,** 547-581.

Bennett, J. W. and Klich, M. (2003) Mycotoxins. *Clin Microbiol Rev,* **16,** 497-516.

Boenisch, M. J., Broz, K. L., Purvine, S. O., Chrisler, W. B., Nicora, C. D., Connolly, L. R. Freitag, M. Baker, S. E. and Kistler, H. C. (2017) Structural reorganization of the fungal endoplasmic reticulum upon induction of mycotoxin biosynthesis. *Sci Rep,* **7,** 44296.

Bonnighausen, J., Gebhard, D., Kroger, C., Hadeler, B., Tumforde, T., Lieberei, R., Bergemann, J., Schafer, W. and Bormann, J. (2015) Disruption of the GABA shunt affects mitochondrial respiration and virulence in the cereal pathogen *Fusarium graminearum*. *Mol Microbiol,* **98,** 1115-1132.

Boutigny, A. L., Barreau, C., Atanasova-Penichon, V., Verdal-Bonnin, M. N., Pinson-Gadais, L. and Richard-Forget, F. (2009) Ferulic acid, an efficient inhibitor of type B trichothecene biosynthesis and Tri gene expression in *Fusarium* liquid cultures. *Mycol Res,* **113,** 746-753.

Cappelli.Ra and Peterson, J. L. (1965) Macroconidium formation in submerged cultures by a non-sporulating strain of *Gibberella Zeae*. *Mycologia,* **57,** 962-+.

Desjardins, A. E. (2006) Fusarium Mycotoxins: chemistry, genetics, and biology *APS Press, St. Paul, Minnesota, USA*

Desjardins, A. E., Hohn, T. M. and Mccormick, S. P. (1993) Trichothecene biosynthesis in *Fusarium* Species - chemistry, genetics, and significance.

Microbiol Rev, **57,** 595-604.

Dimmer, K. S., Fritz, S., Fuchs, F., Messerschmitt, M., Weinbach, N., Neupert, W., *et al.* (2002a) Genetic basis of mitochondrial function and morphology in *Saccharomyces cerevisiae*. *Mol Biol Cell,* **13,** 847-853.

Dimmer, K. S., Fritz, S., Fuchs, F., Messerschmitt, M., Weinbach, N., Neupert, W. and Westermann, B. (2002b) Genetic basis of mitochondrial function and morphology in Saccharomyces cerevisiae. *Mol Biol Cell,* **13,** 847-853.

Dimmer, K. S., Navoni, F., Casarin, A., Trevisson, E., Endele, S., Winterpacht, A., Salviati, L. and Scorrano, L. (2008) LETM1, deleted in Wolf-Hirschhorn syndrome is required for normal mitochondrial morphology and cellular viability. *Hum Mol Genet,* **17,** 201-214.

Dong, F., Qiu, J., Xu, J., Yu, M., Wang, S., Sun, Y., Zhang, G. and Shi, J. (2016) Effect of environmental factors on *Fusarium* population and associated trichothecenes in wheat grain grown in Jiangsu province, China. *Int J Food Microbiol,* **230,** 58-63.

Endele, S., Fuhry, M., Pak, S. J., Zabel, B. U. and Winterpacht, A. (1999) LETM1, a novel gene encoding a putative EF-hand Ca^{2+}-binding protein, flanks the Wolf-Hirschhorn syndrome (WHS) critical region and is deleted in most WHS patients. *Genomics,* **60,** 218-225.

Frazier, A. E., Taylor, R. D., Mick, D. U., Warscheid, B., Stoepel, N., Meyer, H. E., Ryan, M. T., Guiard, B. and Rehling, P. (2006) Mdm38 interacts with ribosomes and is a component of the mitochondrial protein export machinery. *J Cell Biol,* **172,** 553-564.

Gardiner, D. M., Kazan, K. and Manners, J. M. (2009) Nutrient profiling reveals potent inducers of trichothecene biosynthesis in *Fusarium graminearum*. *Fungal Genet Biol,* **46,** 604-613.

Grissa, I., Bidard, F., Grognet, P., Grossetete, S. and Silar, P. (2010) The

Nox/Ferric reductase/Ferric reductase-like families of Eumycetes. *Fungal Biol,* **114,** 766-777.

Gu, Q., Chen, Y., Liu, Y., Zhang, C. and Ma, Z. H. (2015a) The transmembrane protein FgSho1 regulates fungal development and pathogenicity via the MAPK module Ste50-Ste11-Ste7 in *Fusarium graminearum*. *New Phytol,* **206,** 315-328.

Gu, Q., Zhang, C., Liu, X. and Ma, Z. H. (2015b) A transcription factor FgSte12 is required for pathogenicity in *Fusarium graminearum. Mol plant pathol,* **16,** 1-13.

Hasegawa, A. and van der Bliek, A. M. (2007) Inverse correlation between expression of the Wolfs Hirschhorn candidate gene Letm1 and mitochondrial volume in *C. elegans* and in mammalian cells. *Hum Mol Genet,* **16,** 2061-2071.

Hashimi, H., McDonald, L., Stribrna, E. and Lukes, J. (2013) Trypanosome Letm1 protein Is essential for mitochondrial potassium homeostasis. *J Biol Chem,* **288,** 26914-26925.

He, X. J. and Fassler, J. S. (2005) Identification of novel Yap1p and Skn7p binding sites involved in the oxidative stress response of *Saccharomyces cerevisiae*. *Mol Microbiol*, **58,** 1454-1467.

Heller, J. and Tudzynski, P. (2011) Reactive oxygen species in phytopathogenic fungi: signaling, development, and disease. *Annu Rev Phytopathol, Vol 49,* **49,** 369-390.

Hocking, A. D. (1989) Responses of fungi to modified atmospheres. In: *Fumigation and Controlled Atmosphere Storage of Grain, Proceedings of an International Conference Held at Singapore.* pp. 14-18.

Hu, S., Zhou, X. Y., Gu, X. Y., Cao, S. L., Wang, C. F. and Xu, J. R. (2014) The cAMP-PKA pathway regulates growth, sexual and asexual differentiation, and pathogenesis in *Fusarium graminearum*. *Mol Plant Microbe In*, 27, 557-566.

Hwang, S. K., Piao, L., Lim, H. T., Minai-Tehrani, A., Yu, K. N., Ha, Y. C., Chae, C. H., Lee, K. H., Beck, G. R., Park, J. and Cho, M. H. (2010) Suppression of

lung tumorigenesis by Leucine Zipper/EF Hand-containing transmembrane-1. *PLoS One,* **5**.

Ji, F., Xu, J., Liu, X., Yin, X. and Shi, J. (2014) Natural occurrence of deoxynivalenol and zearalenone in wheat from Jiangsu province, China. *Food Chem,* **157,** 393-397.

Jiang, C., Zhang, C., Wu, C., Sun, P., Hou, R., Liu, H. and Xu, J. R. (2016) TRI6 and TRI10 play different roles in the regulation of deoxynivalenol (DON) production by cAMP signalling in *Fusarium graminearum*. *Environ Microbiol,* **18,** 3689-3701.

Jiang, C., Zhang, S. J., Zhang, Q., Tao, Y., Wang, C. F. and Xu, J. R. (2015) FgSKN7 and FgATF1 have overlapping functions in ascosporogenesis, pathogenesis and stress responses in *Fusarium graminearum*. *Environ Microbiol,* **17,** 1245-1260.

Jiang, J., Liu, X., Yin, Y. and Ma, Z. H. (2011) Involvement of a velvet protein FgVeA in the regulation of asexual development, lipid and secondary metabolisms and virulence in *Fusarium graminearum*. *PLoS One,* **6,** e28291.

Jiao, F., Kawakami, A. and Nakajima, T. (2008) Effects of different carbon sources on trichothecene production and Tri gene expression by *Fusarium graminearum* in liquid culture. *FEMS Microbiol Let,* **285,** 212-219.

Kim, D. and Hahn, J. S. (2013) Roles of the Yap1transcription factor and antioxidants in *Saccharomyces cerevisiae*'s Ttolerance to furfural and 5-Hydroxymethylfurfural, which function as thiol-reactive electrophiles generating oxidative stress. *Appl Environ Microbiol,* **79,** 5069-5077.

Kimura, M., Anzai, H. and Yamaguchi, I. (2001) Microbial toxins in plant-pathogen interactions: biosynthesis, resistance mechanisms, and significance. *J Gen Appl Microbiol,* **47,** 149-160.

Kimura, M., Tokai, T., Takahashi-Ando, N., Ohsato, S. and Fujimura, M. (2007) Molecular and genetic studies of *Fusarium* trichothecene biosynthesis: Pathways,

genes, and evolution. *Biosci Biotech and Bioch,* **71,** 2105-2123.

Liu, S. S. (1999) Cooperation of a "reactive oxygen cycle" with the Q cycle and the proton cycle in the respiratory chain - Superoxide generating and cycling mechanisms in mitochondria. *J Bioenerg Biomembr,* **31,** 367-376.

Liu, X., Jiang, J.H, Yin Y.N and Ma, Z. H. (2013) Involvement of FgERG4 in ergosterol biosynthesis, vegetative differentiation and virulence in *Fusarium graminearum. Mol Plant Pathol*. **14**(1):71-83.

Liu, Y., Liu, N., Yin, Y. N., Chen, Y., Jiang, J. H. and Ma, Z. H. (2015) Histone H3K4 methylation regulates hyphal growth, secondary metabolism and multiple stress responses in *Fusarium graminearum*. *Environ Microbiol,* **17,** 4615-4630.

Livak, K. J. and Schmittgen, T. D. (2001) Analysis of relative gene expression data using real-time quantitative PCR and the $2^{-\Delta\Delta CT}$ method. *Methods,* **25,** 402-408.

McQuibban, A. G., Joza, N., Megighian, A., Scorzeto, M., Zanini, D., Reipert, S., Richter, C., Schweyen, R. J. and Nowikovsky, K. (2010) A *Drosophila* mutant of LETM1, a candidate gene for seizures in Wolf-Hirschhorn syndrome. *Hum Mol Gen,* **19,** 987-1000.

Menke, J., Dong, Y. and Kistler, H. C. (2012) *Fusarium graminearum* Tri12p influences virulence to wheat and trichothecene accumulation. *Mol Plant Microbe Interact,* **25,** 1408-1418.

Mentges, M. and Bormann, J. (2015) Real-time imaging of hydrogen peroxide dynamics in vegetative and pathogenic hyphae of *Fusarium graminearum*. *Sci Rep*, **5**, 14980.

Merhej, J., Richard-Forget, F. and Barreau, C. (2011) The pH regulatory factor Pac1 regulates Tri gene expression and trichothecene production in *Fusarium graminearum*. *Fungal Genet Biol,* **48,** 275-284.

Miller, J. D. and Greenhalgh, R. (1985) Nutrient effects on the biosynthesis of trichothecenes and other metabolites by *Fusarium graminearum*. *Mycologia,* **77,**

130-136.

Missall, T. A., Lodge, J. K. and McEwen, J. E. (2004) Mechanisms of resistance to oxidative and nitrosative stress: Implications for fungal survival in mammalian hosts. *Eukaryot Cell,* **3,** 835-846.

Montibus, M., Ducos, C., Bonnin-Verdal, M. N., Bormann, J., Ponts, N., Richard-Forget, F. and Barreau, C. (2013) The bZIP transcription factor Fgap1 mediates oxidative stress response and trichothecene biosynthesis but not virulence in *Fusarium graminearum*. *PLoS One,* **8**.

Nowikovsky, K., Froschauer, E. M., Zsurka, G., Samaj, J., Reipert, S., Kolisek, M., Wiesenberger, G. and Schweyen, R. J. (2004) The LETM1/YOL027 gene family encodes a factor of the mitochondrial K^+ homeostasis with a potential role in the Wolf-Hirschhorn syndrome. *J Biol Chem,* **279,** 30307-30315.

Oh, M., Son, H., Choi, G. J., Lee, C., Kim, J. C., Kim, H. and Lee Y. W. (2016) Transcription factor ART1 mediates starch hydrolysis and mycotoxin production in *Fusarium graminearum* and *F. verticillioides*. *Mol Plant Pathol*, 17(5):755-768.

Osiewacz, H. D. (2002) Mitochondrial functions and aging. *Gene,* **286,** 65-71.

Paster, N., Barkal G. R, and Calderon, M (1986) Control of T-2 toxin production using atmospheric gases. *J Food Protect,* **49,** 615-617.

Paster, N. and Lisker, N. (1985) Effects of controlled atmospheres on *Penicillium patulum* growth and patulin production. *Trichothecenes and Other Mycotoxins (J. Lacy, ed.), New York: John Wiley and Sons*.

Pinson-Gadais, L., Richard-Forget, F., Frasse, P., Barreau, C., Cahagnier, B., Richard-Molard, D. and Bakan, B. (2008) Magnesium represses trichothecene biosynthesis and modulates *Tri5*, *Tri6*, and *Tri12* genes expression in *Fusarium graminearum*. *Mycopathologia,* **165,** 51-59.

Ponts, N., Pinson-Gadais, L., Barreau, C., Richard-Forget, F. and Ouellet, T. (2007) Exogenous H_2O_2 and catalase treatments interfere with Tri genes

expression in liquid cultures of *Fusarium graminearum*. *FEBS Let,* **581,** 443-447.

Ponts, N., Pinson-Gadais, L., Verdal-Bonnin, M. N., Barreau, C. and Richard-Forget, F. (2006) Accumulation of deoxynivalenol and its 15-acetylated form is significantly modulated by oxidative stress in liquid cultures of *Fusarium graminearum*. *FEMS Microbiol Let,* **258,** 102-107.

Raitt, D. C., Johnson, A. L., Erkine, A. M., Makino, K., Morgan, B., Gross, D. S. and Johnston, L. H. (2000) The Skn7 response regulator of *Saccharomyces cerevisiae* interacts with Hsf1 in vivo and is required for the induction of heat shock genes by oxidative stress. *Mol Bio Cell,* **11,** 2335-2347.

Schlickum, S., Moghekar, A., Simpson, J. C., Steglich, C., O'Brien, R. J., Winterpacht, A. and Endele, S. U. (2004) LETM1, a gene deleted in Wolf-Hirschhorn syndrome, encodes an evolutionarily conserved mitochondrial protein. *Genomics,* **83,** 254-261.

Sickmann, A., Reinders, J., Wagner, Y., Joppich, C., Zahedi, R., Meyer, H. E., Schonfisch, B.., Perschil, I., Chacinska, A., Guiard, B., Rehling, P., Pfanner, N.and Meisinger, C. (2003) The proteome of *Saccharomyces cerevisiae* mitochondria. *Proc. Natl. Acad. Sci. USA,* **100,** 13207-13212.

Sinha, H., David, L., Pascon, R. C., Clauder-Munster, S., Krishnakumar, S., Nguyen, M., Shi, G., Dean, J., Davis, R. W., Oefner, P. J., McCusker, J. H. and Steinmetz, L. M. (2008) Sequential elimination of major-effect contributors identifies additional quantitative trait loci conditioning high-temperature growth in yeast. *Genetics,* **180,** 1661-1670.

Tamai, S., Iida, H., Yokota, S., Sayano, T., Kiguchiya, S., Ishihara, N. (2008) Characterization of the mitochondrial protein LETM1, which maintains the mitochondrial tubular shapes and interacts with the AAA-ATPase BCS1L. *J Cell Sci,* **121,** 2588-2600.

Van Nguyen, T., Kroger, C., Bonnighausen, J., Schafer, W. and Bormann, J.

(2013) The ATF/CREB transcription factor Atf1 is essential for full virulence, deoxynivalenol production, and stress tolerance in the cereal pathogen *Fusarium graminearum*. *Mol Plant-Microbe Interact,* **26,** 1378-1394.

Wang, L., Mogg, C., Walkowiak, S., Joshi, M. and Subramaniam, R. (2014) Characterization of NADPH oxidase genes NoxA and NoxB in *Fusarium graminearum*. *Can J Plant Pathol,* **36,** 12-21.

Yun, Y. Z., Liu, Z. Y., Yin, Y. N., Jiang, J. H., Chen, Y., Xu, J. R. and Ma Z. H. (2015) Functional analysis of the *Fusarium graminearum* phosphatome. *New Phytol,* **207,** 119-134.

Zhang, B. T., Carrie, C., Ivanova, A., Narsai, R., Murcha, M. W., Duncan, O.*, et al.* (2012) LETM proteins play a role in the accumulation of mitochondrially encoded proteins in *Arabidopsis thaliana* and AtLETM2 displays parent of origin effects. *J Biol Chem,* **287,** 41757-41773.

Zhang, C., Lin, Y., Wang, J., Wang, Y., Chen, M., Norvienyeku, J., Li, G., Yu, W. and Wang, Z. H. (2016) FgNoxR, a regulatory subunit of NADPH oxidases, is required for female fertility and pathogenicity in *Fusarium graminearum*. *FEMS Microbiol Let,* **363,** fnv223.

Zollino, M., Lecce, R., Fischetto, R., Murdolo, M., Faravelli, F., Selicorni, A., Butte, C., Memo, L., Capovilla, G. and Neri, G. (2003) Mapping the Wolf-Hirschhorn syndrome phenotype outside the currently accepted WHS critical region and defining a new critical region, WHSCR-2. *Am J Hum Genet,* **72,** 590-597.

Figure legends

Fig. 1. Identification of the Letm1-like proteins in *Fusarium graminearum*. **a**. Schematic architecture of the Letm1 super-family proteins in *F. graminearum*, FgLetm1 and FgLetm2. The *Homo sapiens* Letm1 and *S. cerevisiae* Mdm38 and Ylh47 are selected as references. Conserved domains are indicated. **b**. Phylogenetic analysis of the putative Letm1-like proteins from *F. graminearum* and six plant pathogenic fungi. Amino acid sequences of the Letm1 orthologs are aligned using Clustal W and a neighbor-joining tree generated by MEGA 5.0. **c**. Transcriptional levels of the *FgLETM1* and *FgLETM2* genes in the CMC, hyphae, infected plant tissues and TBI by RNA-seq.

Fig. 2. Phenotypes of the deletion mutants of ΔFgLetm1, ΔFgLetm2 and ΔΔFgLetm1/2 in vegetative growth, conidiogenesis and germination. **a**. Colony morphology of PH-1, the mutants and the complemented strains on PDA and MM at 25 °C for 3 days. **b**. Ratio of the different number of conidial septa in PH-1, mutants and complemented strains harvested from 5-day-old CMC cultures. **c**. ΔFgLetm1 reduced the conidial germination. The column labeled with star indicates a significant difference at $P = 0.05$.

Fig. 3. ΔFgLetm1 increased the sensitivity towards osmotic stress, heat shock, fungicides and ion stresses. **a**. Growth phenotype of PH-1, mutants and complemented strains grown on MM without or with supplementation of NaCl or KCl after 4 days of incubation at 25 °C. **b**. Statistical analysis of the growth inhibition rate of all strains under the osmotic stresses. **c**. ΔFgLetm1 increased the sensitivity toward high temperature. Colony morphology was shown after 4 days of incubation on MM

at 15 °C and 25 °C, and 7 days of incubation at 32 °C. **d**. The transcriptional level of the heat tolerant genes *FgHSP30*, *FgHSP70* and *FgGSY2* decreased in the ΔFgLetm1 mutant in response to heat shock, in comparison to that in PH-1. The expression levels of each gene at 25 °C for 16 h were set to 1. **e**. The ΔFgLetm1 mutant was more sensitive towards fungicides iprodione, phenamacril, and ion stresses than that of the wild type. Plates were incubated at 25 °C for 4 days before imaging. **f**. Statistical analysis of the growth inhibition rate of strains towards above stresses. Values on the bars followed by the same letter mean no significant difference at $P = 0.05$.

Fig. 4. FgLetm1 is localized to mitochondria and critical for the mitochondrial integrity.

a. Both FgLetm1 and FgLetm2 are localized to the mitochondria. Mycelia of FgLetm1-C and FgLetm2-C were grown in CM and stained with Mito-HcRed. Images were taken by confocal fluorescent microscope. Bar=10 μm. b. ΔFgLetm1 changed the mitochondrial structural patterns. Strains were grown in CM broth for 16 h at 25 °C, then harvested and stained with Mito-HcRed for observation. Typical patterns in individual strain were shown. Bar= 10 μm. **c**. ΔFgLetm1 mutant caused mitochondrial swelling. Ultrastructural morphology of mitochondria in each strain was visualized by transmission electron microscope. Bars were indicated in images. **d**. ΔFgLetm1 decreased the protein level of cytochrome *b* (Cyt *b*), an indicator protein of respiratory chain components. The protein abundance of Cyt *b* in the PH-1 and mutants were analyzed by immunoblot assays. The histone H3 was used as a reference protein.

Fig. 5. Deletion mutant of ΔFgLetm1 decreased the concentration of

endogenous reactive oxygen species (ROS).

a. ΔFgLetm1 strongly reduced the endogenous ROS in MM and TBI. Hyphae grown in MM for 24 h, or TBI for 3 days were stained by the ROS indicator, H2DCFDA. Bar=10 μm. **b**. Mutant of ΔFgLetm1 and ΔΔFgLetm1/2 decreased the transcriptional level of genes encoding catalases and superoxide dismutases in TBI. **c**. Mutant of ΔFgLetm1 and ΔΔFgLetm1/2 increased the resistance towards the oxidative stress by H_2O_2. Strains were grown on MM with or without 10 mM H_2O_2 for 4 days at 25°C. **d**. Statistical analysis of the growth inhibition rate of PH-1, mutants and complemented strains towards the oxidative stress generated by H_2O_2. Values on the bars followed by the same letter indicate no significant difference at $P = 0.01$.

Fig. 6 Deletion mutants of ΔFgLetm1 and ΔΔFgLetm1/2 were attenuated in virulence *in planta*.

a. Dissection of infected wheat heads caused by PH-1, the mutants and the complemented strains. Inoculated ears were dissected at 15 dpi. Inoculated sites were indicated with red arrows. **b**. Infection structures on glumes infected by PH-1, mutants and complemented strains. The inoculated glumes were collected after 2 dpi with conidia, and observed by SEM. The infection structures were pointed out by red arrows, and details were enlarged.

Fig. 7. Deletion mutants of ΔFgLetm1 and ΔΔFgLetm1/2 reduced the DON biosynthesis *in vitro* and *in planta*.

a. ΔFgLetm1 significantly decreased the transcriptional level of *TRI* genes in TBI medium. **b**. Toxisome formation of PH-1, ΔFgLetm1 and ΔFgLetm2. Strains were labeled with Tri1-GFP and incubated in TBI for 3 days, and toxisomes were observed by confocal fluorescent microscope. Bar=10 μm. **c**.

Induction of DON biosynthesis by H_2O_2 in wild type and ΔFgLetm1 grown in LTB medium. H_2O_2 was added into LTB daily, and the supernatant after 7 days of incubation was used for the quantification of DON production. **d**. Relative expression levels of *TRI5*, *TRI6* and *TRI10* in PH-1 and ΔFgLetm1 with or without H_2O_2 treatment. The relative expression level of each gene in wild type without H_2O_2 treatment was arbitrarily set to 1. Values on the bars followed by the same letter indicate no significant difference at $P = 0.05$.

Fig. 8. DON biosynthesis and virulence were reduced under hypoxia conditions.

a. Colony morphology of wild type grown on PDA in the open air and hypoxia conditions. **b**. Relative expression level of *TRI5*, *TRI6* and *TRI10* in the mycelium of PH-1 under open air and hypoxia conditions. Strains were grown in TBI for 3 days. The pigment biosynthesis gene, *AURJ*, was used as a control. **c**. Toxisome formation of the wild type under open air and hypoxia conditions. The Tri1-GFP was observed after 3 days of incubation. **d**. DON production of wild type under open air and hypoxia conditions after 7 days of incubation. **e**. Virulence of wild type under open air and hypoxia conditions. Scab symptom was taken after 7 dpi.

Supplemental figure, table and video legends

Fig. S1. **Phylogenetic tree of the Letm1 super-family orthologs from 32 fungal genomes available in the NCBI Bioprojects and Broad Institute databases.** Orthologs were retrieved with the yeast Letm1 proteins, Mdm38 and Ylh47, and FgLetm1 and FgLetm2 protein sequences as queries. The phylogenetic tree was constructed by the neighbor-joining method using MEGA 5.0. Numbers at the node represent the results of 1000 bootstrap replications. The GenBank or organism-specific accession numbers are indicated in the figure.

Fig. S2. **Identification of deletion mutants and complemented strains.** **a**. Southern blot hybridization analysis of the deletion mutant of ΔFgLetm1, ΔΔFgLetm1/2, and the complemented strain ΔFgLetm1+P_{LETM1} FgLetm1-GFP using downstream DNA fragments of *FgLETM1* as the probe. Both ΔFgLetm1 and ΔΔFgLetm1/2 had an anticipated 4594 bp band, but both of them lacked the 2219 bp band present in wild-type PH-1, when probed with a 725 bp downstream DNA fragment of *FgLETM1*. **b**. Southern blot hybridization analysis of the deletion mutant of ΔFgLetm2, ΔΔFgLetm1/2, and the complemented strain ΔFgLetm2+P_{LETM2} FgLetm2-GFP using a downstream DNA fragment of *FgLETM2* as the probe. Using an 800 bp upstream DNA fragment of *FgLETM2* as the probe, ΔFgLetm2 mutant had an anticipated 3253 bp band, when the chromosomal DNA of ΔFgLetm2 was digested with *NdeI*. ΔΔFgLetm1/2 presented a 4098 bp band but lacked the 1585 bp band present in the wild-type PH-1, when the chromosomal DNA of ΔΔFgLetm1/2 was digested with *EcoRV* and blotted with the same probe. **c**. PCR verification of complemented strain ΔFgLetm1+P_{LETM1} FgLetm1-GFP, and

ΔFgLetm2+P_{LETM2} FgLetm2-GFP. The whole cassette including the promoter, ORF and gfp was amplified, respectively.

Fig. S3. **Conidial morphology of the wild type, ΔFgLetm1, ΔFgLetm2, ΔΔFgLetm1/2 and the complemented strains. T**he septa were stained with calcofluor white and observed by fluorescent microscope. Bar= 20 μm.

Fig. S4. Colony morphology of PH-1, the mutants and the complemented strains on wheat head medium (WA) at 25 °C for 3 days.

Fig. S5. **Infection structure of wild type and deletion mutant of ΔFgLetm1 on the inoculated glumes at 14 days post-inoculation.** Samples were collected after 2 weeks post-inoculation and observed by the scan electron microscope. Bars were indicated on the images.

Fig. S6. **Induction of DON biosynthesis by exogenous ATP in the wild type and mutants grown in TBI medium.** ATP was added into TBI with at the final concentration of 10 μM, and the cell free supernatant after 7 days of incubation was used for the quantification of DON production. Error bars denote standard deviation from three repeated experiments.

Fig. S7. Deletion mutant of ΔFgLetm1 was not changed the utilization of non-fermentable carbon. Colony morphology of the wild type, ΔFgLetm1, ΔFgLetm2 and ΔΔFgLetm1/2 on minimal medium supplemented with glucose or glycerol as a sole carbon source. Plates were photographed after incubation at 25 °C for 3 days.

Fig. S8. Fungicides targeting mitochondria are able to inhibit the toxisome formation and DON biosynthesis.

a. The growth inhibition of tested fungicides at 0.3 μg/ml. **b**. Toxisome formation of fungicides at 0.3 μg/ml. The ΔTri1:Tri1-GFP strain was grown in

TBI for 24 h, then individual fungicide was added at the final concentration at 0.3 μg/ml and incubated for another 24 h before observation. **c**. The DON production of each treatment. The DON was extracted from the 7-day cultured TBI in each treatment and quantified by LC-MS. Column followed by different letter indicated a significantly difference at $P = 0.05$.

Table S1 The Letm1-superfamily domain in the Letm1 orthologues of 6 filamentous plant pathogenic fungi and *Saccharomyces cerevisiae*.

Table S2 Proteins of the mitochondrial ribosome in complex with FgLetm1 by affinity purification and mass spectrometry assay.

Table S3. Oligonucleotide primers used in this study.

Video 1. Mitochondrial patterns stained by Mito-HcRed in the wild type.

Video 2. Mitochondrial patterns stained by Mito-HcRed in deletion mutant of ΔFgLetm1.

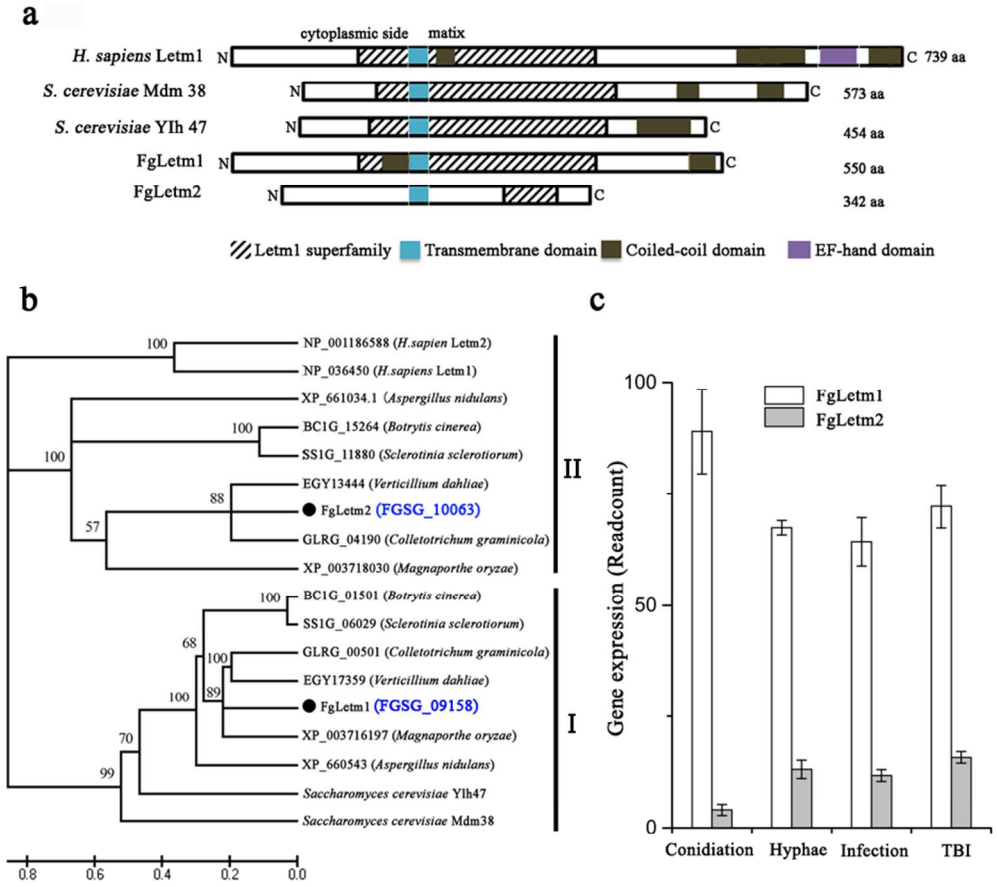

Fig. 1. Identification of the Letm1-like proteins in Fusarium graminearum. a. Schematic architecture of the Letm1 super-family proteins in F. graminearum, FgLetm1 and FgLetm2. The Homo sapiens Letm1 and S. cerevisiae Mdm38 and Ylh47 are selected as references. Conserved domains are indicated. b. Phylogenetic analysis of the putative Letm1-like proteins from F. graminearum and six plant pathogenic fungi. Amino acid sequences of the Letm1 orthologs are aligned using Clustal W and a neighbor-joining tree generated by MEGA 5.0. c. Transcriptional levels of the FgLETM1 and FgLETM2 genes in the CMC, hyphae, infected plant tissues and TBI by RNA-seq.

80x73mm (300 x 300 DPI)

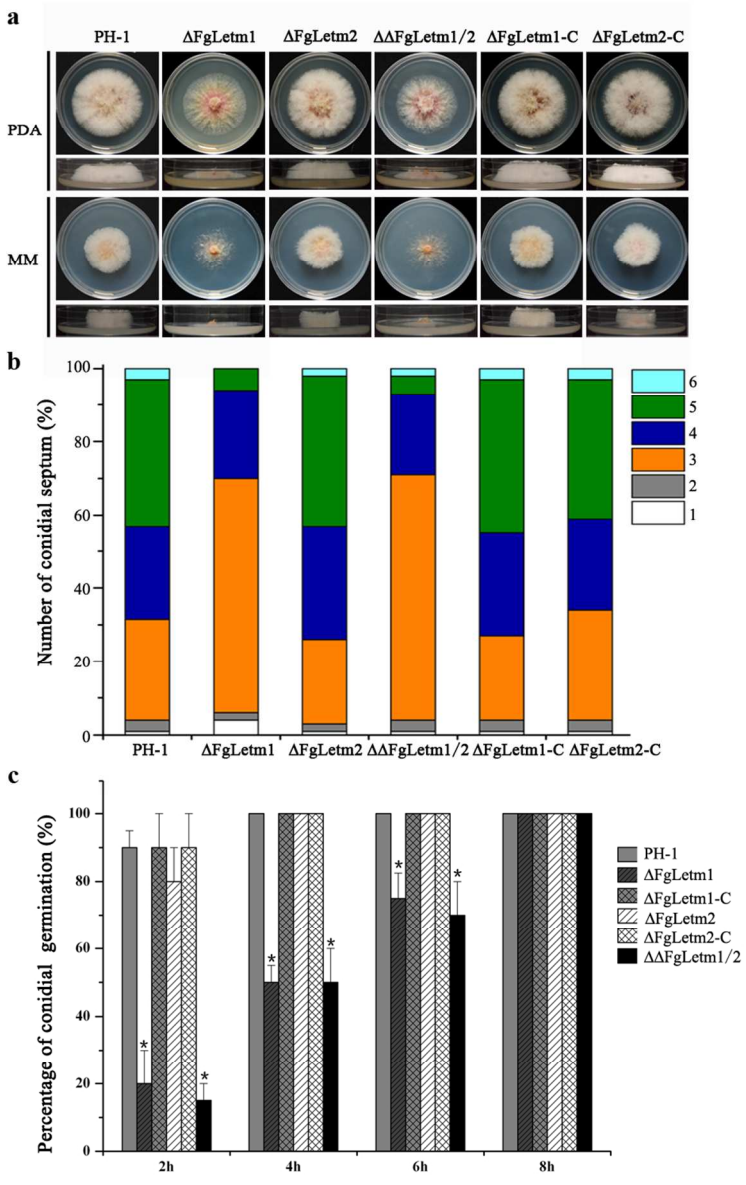

Fig. 2. Phenotypes of the deletion mutants of ΔFgLetm1, ΔFgLetm2 and ΔΔFgLetm1/2 in vegetative growth, conidiogenesis and germination.
a. Colony morphology of PH-1, the mutants and the complemented strains on PDA and MM at 25 °C for 3 days. b. Ratio of the different number of conidial septa in PH-1, mutants and complemented strains harvested from 5-day-old CMC cultures. c.ΔFgLetm1 reduced the conidial germination. The column labeled with star indicates a significant difference at P = 0.05.

80x128mm (300 x 300 DPI)

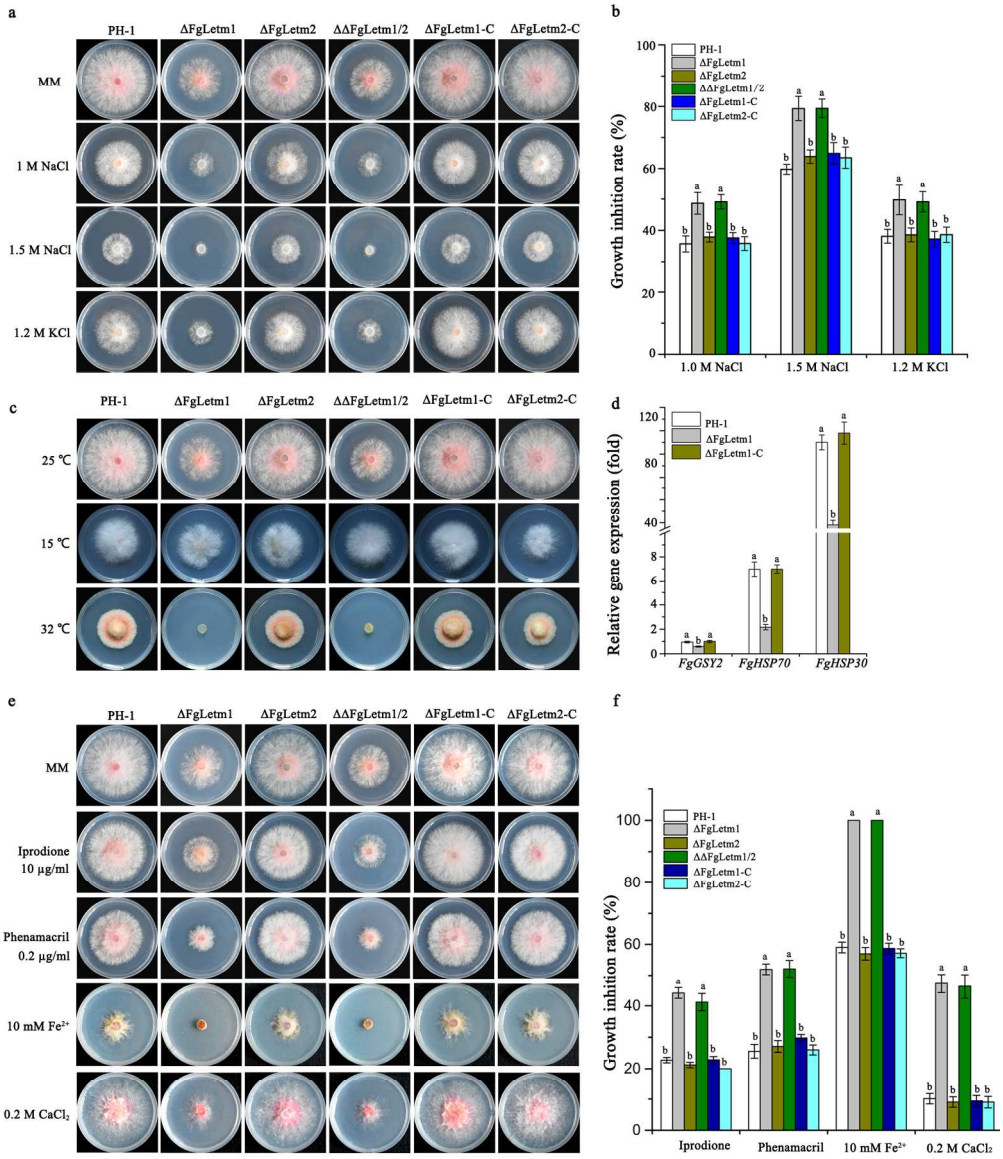

Fig. 3. ΔFgLetm1 increased the sensitivity towards osmotic stress, heat shock, fungicides and ion stresses. a. Growth phenotype of PH-1, mutants and complemented strains grown on MM without or with supplementation of NaCl or KCl after 4 days of incubation at 25 °C. b. Statistical analysis of the growth inhibition rate of all strains under the osmotic stresses. c. ΔFgLetm1 increased the sensitivity toward high temperature. Colony morphology was shown after 4 days of incubation on MM at 15 °C and 25 °C, and 7 days of incubation at 32 °C. d. The transcriptional level of the heat tolerant genes FgHSP30, FgHSP70 and FgGSY2 decreased in the ΔFgLetm1 mutant in response to heat shock, in comparison to that in PH-1. The expression levels of each gene at 25 °C for 16 h were set to 1. e. The ΔFgLetm1 mutant was more sensitive towards fungicides iprodione, phenamacril, and ion stresses than that of the wild type. Plates were incubated at 25 °C for 4 days before imaging. f. Statistical analysis of the growth inhibition rate of strains towards above stresses. Values on the bars followed by the same letter mean no significant difference at P = 0.05.

170x202mm (300 x 300 DPI)

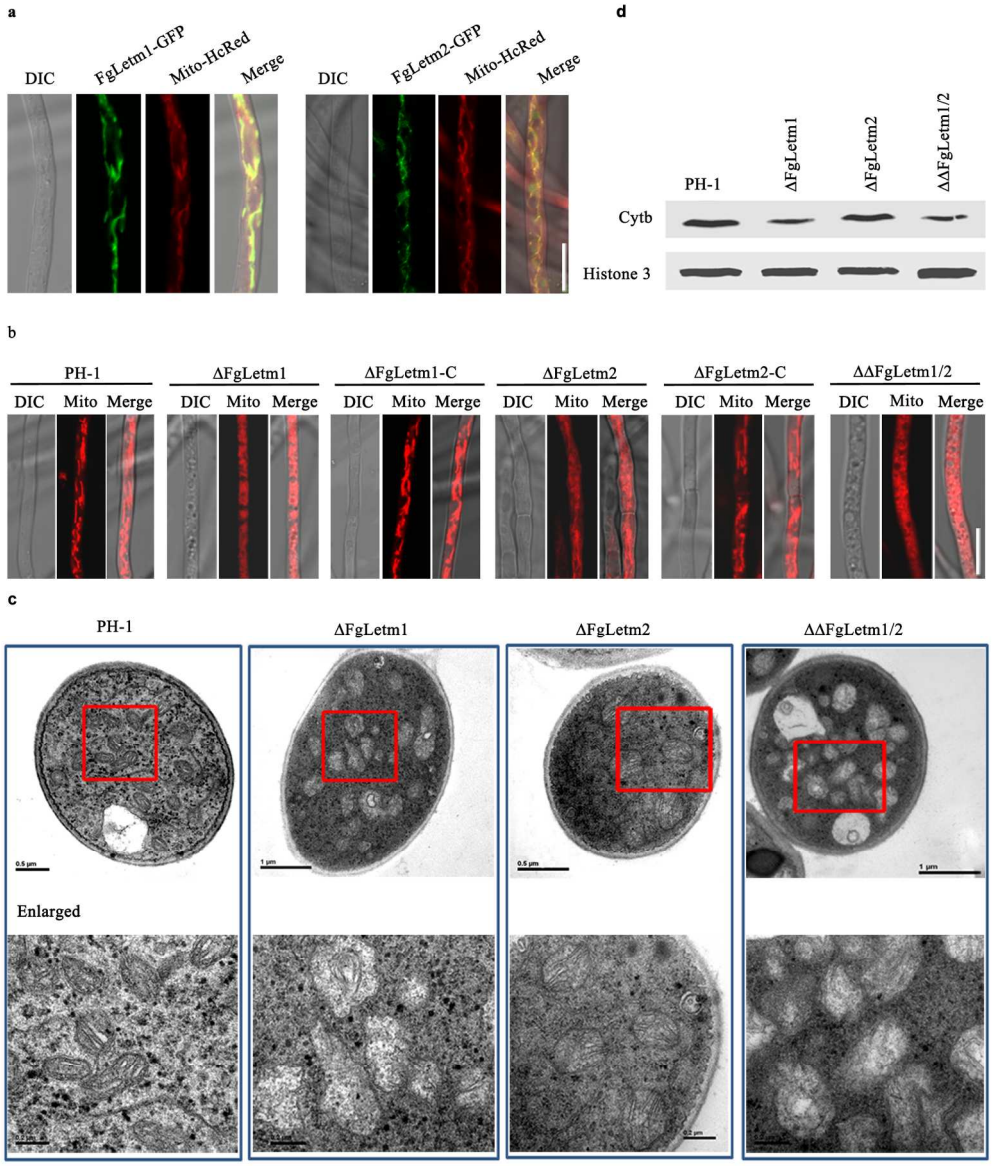

Fig. 4. FgLetm1 is localized to mitochondria and critical for the mitochondrial integrity.
a. Both FgLetm1 and FgLetm2 are localized to the mitochondria. Mycelia of FgLetm1-C and FgLetm2-C were grown in CM and stained with Mito-HcRed. Images were taken by confocal fluorescent microscope. Bar=10 μm. b. ΔFgLetm1 changed the mitochondrial structural patterns. Strains were grown in CM broth for 16 h at 25 °C, then harvested and stained with Mito-HcRed for observation. Typical patterns in individual strain were shown. Bar= 10 μm. c. ΔFgLetm1 mutant caused mitochondrial swelling. Ultrastructural morphology of mitochondria in each strain was visualized by transmission electron microscope. Bars were indicated in images. d. ΔFgLetm1 decreased the protein level of cytochrome b (Cyt b), an indicator protein of respiratory chain components. The protein abundance of Cyt b in the PH-1 and mutants were analyzed by immunoblot assays. The histone H3 was used as a reference protein.

170x200mm (300 x 300 DPI)

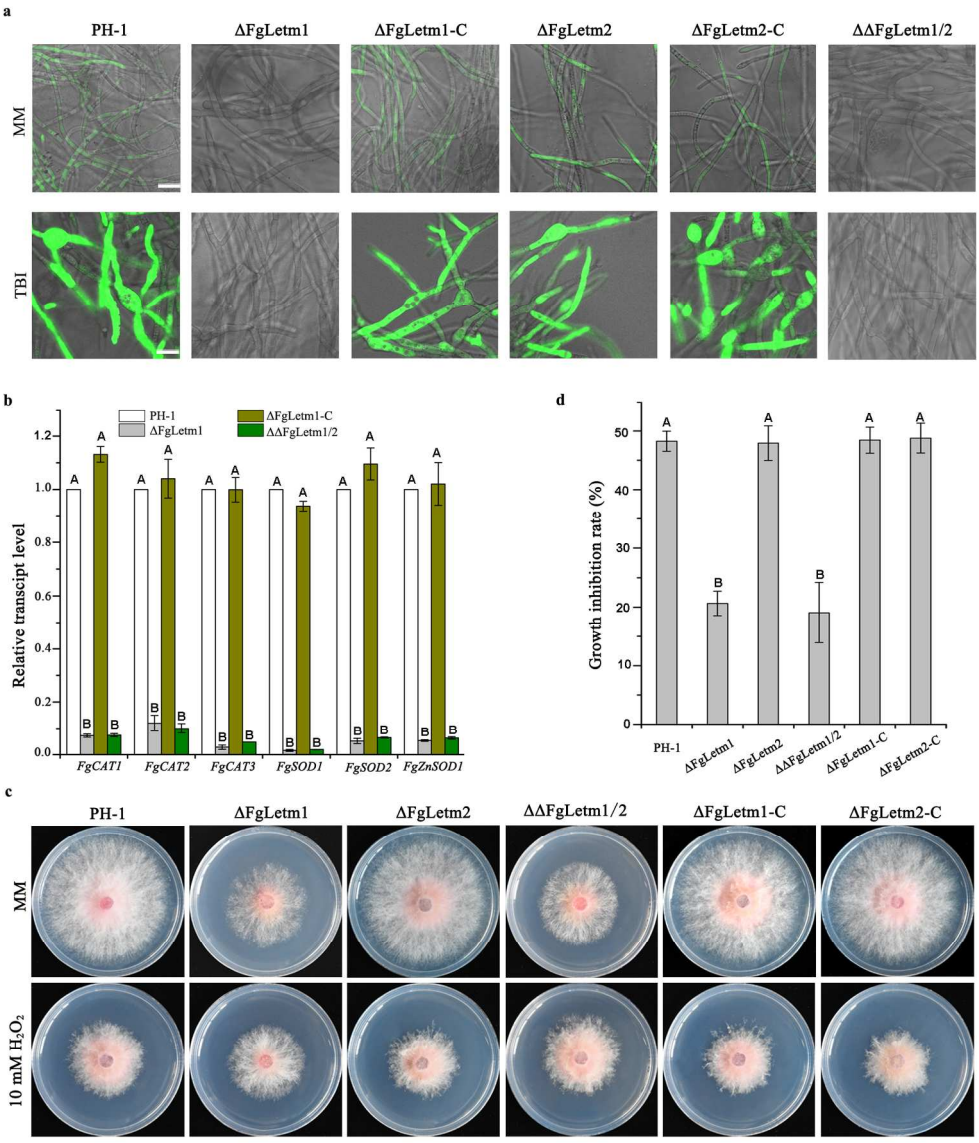

Fig. 5. Deletion mutant of ΔFgLetm1 decreased the concentration of endogenous reactive oxygen species (ROS).

a. ΔFgLetm1 strongly reduced the endogenous ROS in MM and TBI. Hyphae grown in MM for 24 h, or TBI for 3 days were stained by the ROS indicator, H2DCFDA. Bar=10 μm. b. Mutant of ΔFgLetm1 and ΔΔFgLetm1/2 decreased the transcriptional level of genes encoding catalases and superoxide dismutases in TBI. c. Mutant of ΔFgLetm1 and ΔΔFgLetm1/2 increased the resistance towards the oxidative stress by H2O2. Strains were grown on MM with or without 10 mM H2O2 for 4 days at 25°C. d. Statistical analysis of the growth inhibition rate of PH-1, mutants and complemented strains towards the oxidative stress generated by H2O2. Values on the bars followed by the same letter indicate no significant difference at P = 0.01.

170x198mm (300 x 300 DPI)

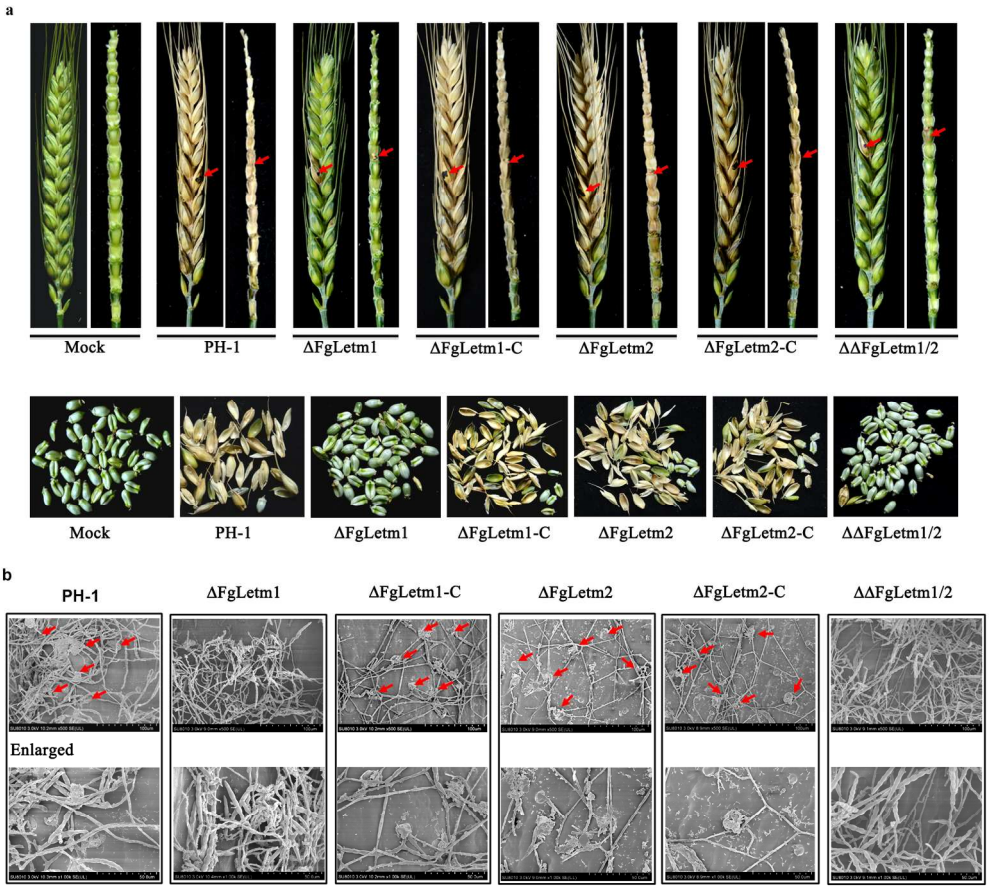

Fig. 6 Deletion mutants of ΔFgLetm1 and ΔΔFgLetm1/2 were attenuated in virulence in planta. a. Dissection of infected wheat heads caused by PH-1, the mutants and the complemented strains. Inoculated ears were dissected at 15 dpi. Inoculated sites were indicated with red arrows. b. Infection structures on glumes infected by PH-1, mutants and complemented strains. The inoculated glumes were collected after 2 dpi with conidia, and observed by SEM. The infection structures were pointed out by red arrows, and details were enlarged.

170x157mm (300 x 300 DPI)

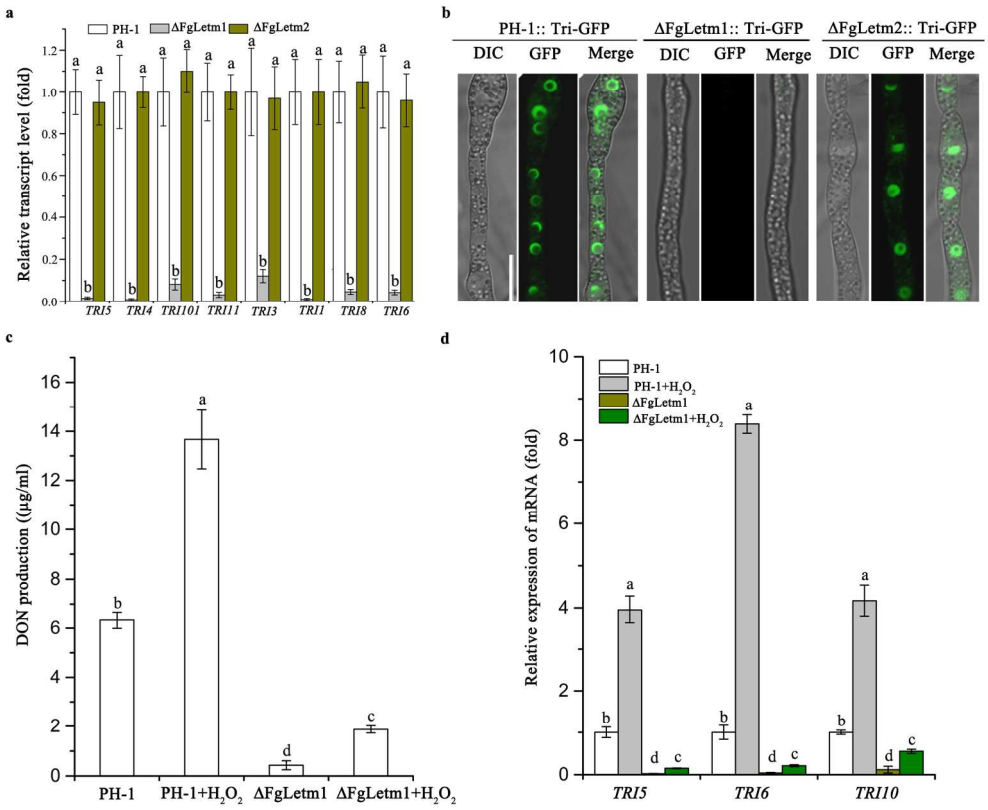

Fig. 7. Deletion mutants of ΔFgLetm1 and ΔΔFgLetm1/2 reduced the DON biosynthesis in vitro and in planta.

a. ΔFgLetm1 significantly decreased the transcriptional level of TRI genes in TBI medium. b. Toxisome formation of PH-1, ΔFgLetm1 and ΔFgLetm2. Strains were labeled with Tri1-GFP and incubated in TBI for 3 days, and toxisomes were observed by confocal fluorescent microscope. Bar=10 μm. c. Induction of DON biosynthesis by H2O2 in wild type and ΔFgLetm1 grown in LTB medium. H2O2 was added into LTB daily, and the supernatant after 7 days of incubation was used for the quantification of DON production. d. Relative expression levels of TRI5, TRI6 and TRI10 in PH-1 and ΔFgLetm1 with or without H2O2 treatment. The relative expression level of each gene in wild type without H2O2 treatment was arbitrarily set to 1. Values on the bars followed by the same letter indicate no significant difference at P = 0.05.

170x143mm (300 x 300 DPI)

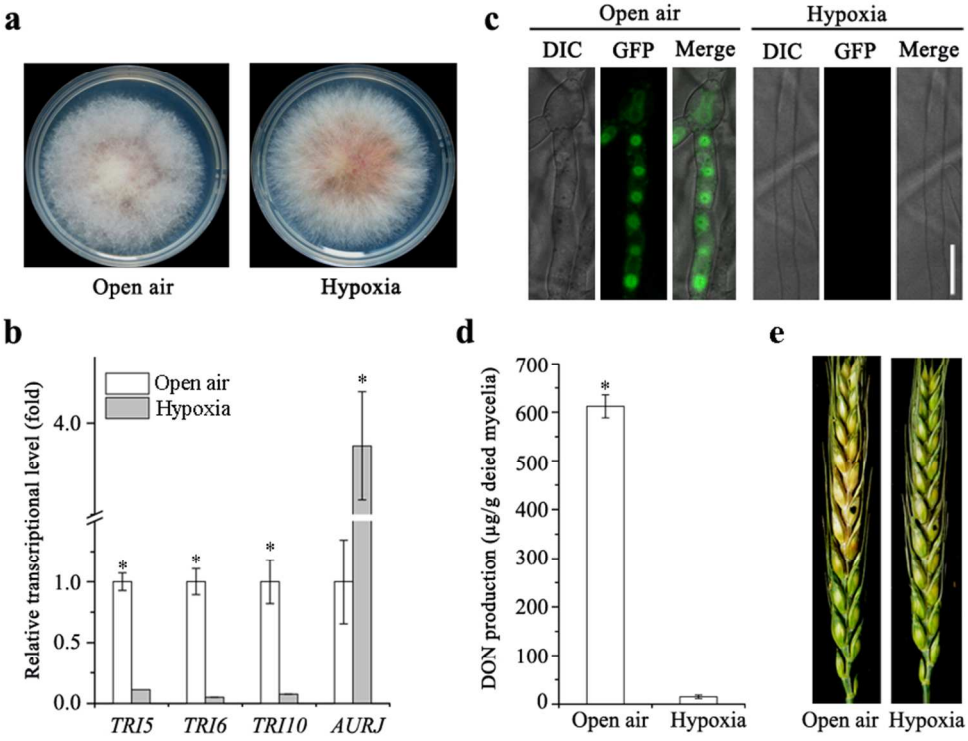

Fig. 8. DON biosynthesis and virulence were reduced under hypoxia conditions.
a. Colony morphology of wild type grown on PDA in the open air and hypoxia conditions. b. Relative expression level of TRI5, TRI6 and TRI10 in the mycelium of PH-1 under open air and hypoxia conditions. Strains were grown in TBI for 3 days. The pigment biosynthesis gene, AURJ, was used as a control. c. Toxisome formation of the wild type under open air and hypoxia conditions. The Tri1-GFP was observed after 3 days of incubation. d. DON production of wild type under open air and hypoxia conditions after 7 days of incubation. e. Virulence of wild type under open air and hypoxia conditions. Scab symptom was taken after 7 dpi.

80x62mm (300 x 300 DPI)

Table 1 Vegetative growth and conidiation of *Fusarium graminearum* strains

Strain	Growth rate (cm/day)	Conidiation Production ($\times 10^5$)	Conidial length (μm)
PH-1	2.43±0.06[a*]	6.15±0.47[a]	63.50±6.10[a]
ΔFgLetm1	2.06±0.03[b]	4.65±0.53[b]	38.88±4.39[b]
Δ FgLetm1-C	2.40±0.04[a]	6.28±0.48[a]	63.13±8.04[a]
Δ FgLetm2	2.32±0.02[a]	6.03±0.38[a]	56.50±5.07[a]
Δ FgLetm2-C	2.37±0.02[a]	5.98±0.26[a]	59.88±2.10[a]
Δ FgLetm12	2.03±0.03[b]	5.20±0.34[b]	41.25±3.57[b]

[*]Values followed by the same letter are not significantly different at $P = 0.05$ for each treatment.

Table 2 Productions of ATP, hydrogen peroxide and ethanol in PH-1, mutants and complemented strains

Strain	ATP (μM)		H_2O_2 (mM)		Ethanol (mg/ml)
	MM	TBI	MM	TBI	MM
PH-1	1341.35±29.24[a*]	1360.05±42.46[a]	24.97±2.14[a]	133.94±9.85[a]	2.16±0.07[b]
ΔFgLetm1	1008.54±34.32[b]	902.17±23.46[b]	3.26±0.18[b]	4.51±0.36[b]	4.32±0.12[a]
Δ FgLetm1-C	1320.14±13.11[a]	1358.23±35.23[a]	20.67±3.25[a]	120.55±20.11[a]	2.3±0.21[b]
Δ FgLetm2	1300.02±24.53[a]	1250.22±48.37[a]	19.66±1.67[b]	122.63±15.37[a]	2.43±0.20[b]
Δ FgLetm2-C	1360.56±15.21[a]	1400.26±68.70[a]	21.79±3.22[a]	120.33±18.54[a]	2.1±0.25[b]
Δ FgLetm12	953.56±30.14[b]	875.65±50.32[b]	2.34±0.86[b]	2.56±0.25[b]	4.17±0.14[a]

[*]Values followed by the same letter are not significantly different at $P = 0.05$ for each treatment.

Table 3 Deoxynivalenol productions of the wild type, mutants and complemented strains in TBI, wheat kernel medium and infected spikelets

	TBI	Wheat kernel	Infected spikelet
Strain	DON production (μg/g dried mycelia)	DON production (μg/mg ergosterol)	DON production (mg/mg ergosterol)
PH-1	650.75±7.07[a*]	398.88±13.07[a]	581.53±30.28[a]
ΔFgLetm1	38.24±2.81[b]	11.81±1.40[b]	228.61±20.25[b]
Δ FgLetm1-C	630.80±12.86[a]	428.56±14.59[a]	536.27±17.36[a]
Δ FgLetm2	635.07±13.80[a]	420.97±15.58[a]	566.54±30.85[a]
Δ FgLetm2-C	660.46±8.96[a]	394.22±15.08[a]	605.03±35.18[a]
Δ FgLetm12	35.93±3.53[b]	9.43±2.89[b]	188.10±19.51[b]

[*]Values followed by the same letter are not significantly different at $P = 0.05$ for each treatment.